Supplementary Information

In section 1 we illustrate the effect of heterogeneities in the rates of populations of independent Poisson process on the ITI distribution. In section 2 we look at the distributions of pairwise coincidences of transitions C_{ij}s. In section 3 we look at the effect of using only a subset of the large data sets to fit the model. In section 4 we discuss our choice of a uniform distribution in the delay. In section 5 we show the equivalent of Fig.1 from the main text for the remaining 14 data sets. In section 6 we provide the fits to the pattern distributions of the 15 data sets from the various models used. For each figure, the data set is indicated by a symbol corresponding to those shown in Fig.2 of the main text.

1 ITI distributions for populations of heterogeneous Poisson processes

The inter-transition-interval distribution (ITI) is a simple analog of the inter-spike-interval distribution. For independent Poisson processes with identical rates we would therefore expect an exponential ITI distribution, with an offset from zero equal to the effective refractory period. However, as can bee seen in Fig.1d and in the analogous ITIs for the remaining 14 data sets, see Figs.S.10-S.23, in no case do we find such an ITI distribution. Rather, in Fig.1d, for increasing ITI one observes a sharp increase round 1 sec, corresponding to the refractory period, followed by a decrease which appears bi-phasic on a log-lin scale, see inset in Fig.1d. An exponential on a log-lin scale would just be a straight line. This effect can be explained by the presence of heterogeneity in the underlying rates of the Poisson processes.

As an example, if the distribution of the Poisson rates $f(p)$ is a uniform distribution from 0 to ϕ and τ is fixed then

$$ITI(z) = \int_0^\infty dp f(p) p e^{-pz} \tag{S.1}$$

$$= \frac{1}{\phi}\left(\frac{1}{z^2}\left(1-e^{-\phi z}\right) - \frac{\phi}{z}e^{-\phi z}\right), \tag{S.2}$$

where $z = t - \tau$. This is qualitatively similar to the ITI distribution seen in Fig.1d, see inset and compare to Fig.S.1.

Here we illustrate the effect of heterogeneity in the underlying rates of a population of Poisson processes by plotting a specific example of Eqs.9 from the *methods* section of the paper, see Fig.S.1.

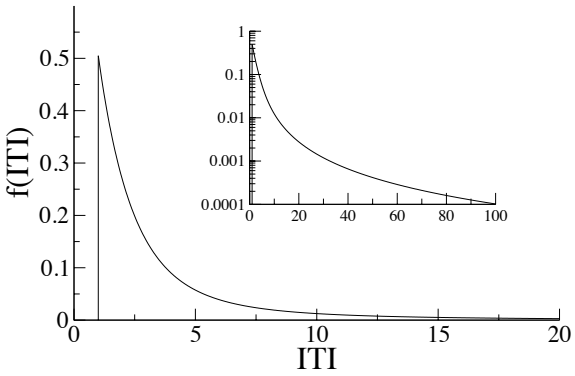

Fig. S.1: Inter-transition-interval distributions for heterogeneous populations of independent Poisson processes. Solid line: Uniform distribution of rates from 0 to 1. Fixed refractory period of 1.

2 The distributions of pairwise coincident transitions, C_{ijs}s

In this section we look at the distributions of the pairwise coincident transitions, C_{ij}s from data sets 1-4. This also provides a graphical interpretation of Eq.2 of the methods sections which sets the values of the excess pairwise transition probabilities p_{ij}s. Fig.S.2 shows the distribution of C_{ij}s for data set 2 (solid bars). It is peaked at zero and monotonically decreasing. The large number of C_{ij}s near zero is due to the sparseness of the data, i.e. small number of transitions. This is typical for all data sets. We can compare the distribution of C_{ij}s extracted from the data to that which one would get from independent Poisson neurons. For data set 2, the non-stationary Poisson model provides a much better fit than the stationary one, so use the data to estimate the rates for nonstationary Poisson neurons. For each neuron pair (i, j), we then find that the probability of finding k coincidences is just

$$P(C_{ij} = k) \;=\; \frac{e^{-\lambda}}{k!}\lambda^k, \tag{S.3}$$

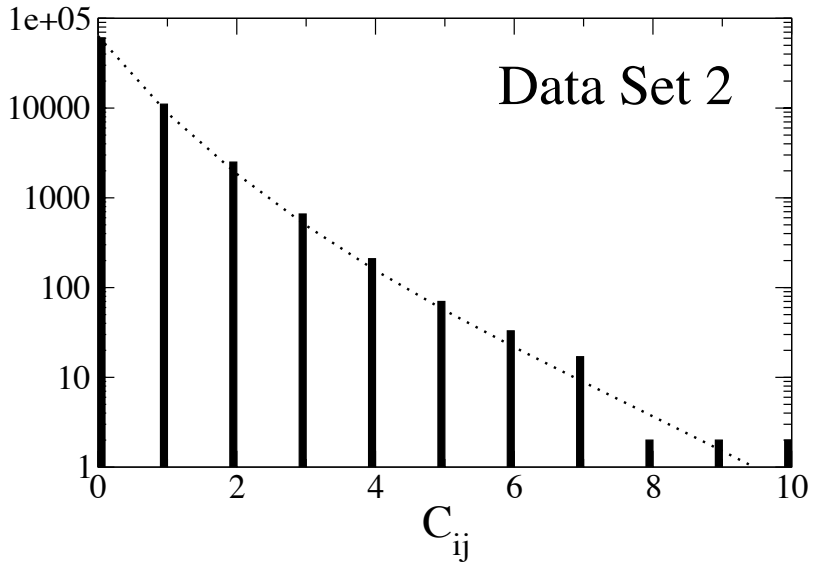

Fig. S.2: The distribution of C_{ij}s for data set 2. The solid bars are the actual number of coincidences while the dotted line is the number of coincidences given independent nonstationary Poisson neurons. See main text for details.

$$\lambda \;=\; (1+w)\sum_{f=1}^{T}\nu_i(f)\nu_j(f), \tag{S.4}$$

where the rate $\nu_i(f)$ is calculated from the data as described in the methods section of the main text. For data sets 1 and 3 we would use the stationary rates for Eq.S.4 since model III gives the best fit. If we now take the sum of all the distributions of pairwise coincidences we obtain the dotted line in Fig.S.2. The agreement with the actual distribution appears quite good. Similar results are obtained for the remaining 3 data sets with interactions (data not shown).

Since we are interested in knowing if some particular neuronal pairs exhibit coincidences beyond what we would expect from Poisson neurons, we can normalize the C_{ij}s in a pairwise way. In particular, we look at the measure $(C_{ij} - E(C_{ij}))/\sigma_{ij}$ where $E(C_{ij}) = \lambda$ and $\sigma_{ij} = \sqrt{E(C_{ij})}$. Fig.S.3 shows the resulting distributions of this measure for data sets 1-4. The insets in Fig.S.3 show the full distributions. The characteristic of the full distributions which most stands out is the large peak at slightly negative values. This occurs because most rates are very low, yielding expected values of C_{ij} between

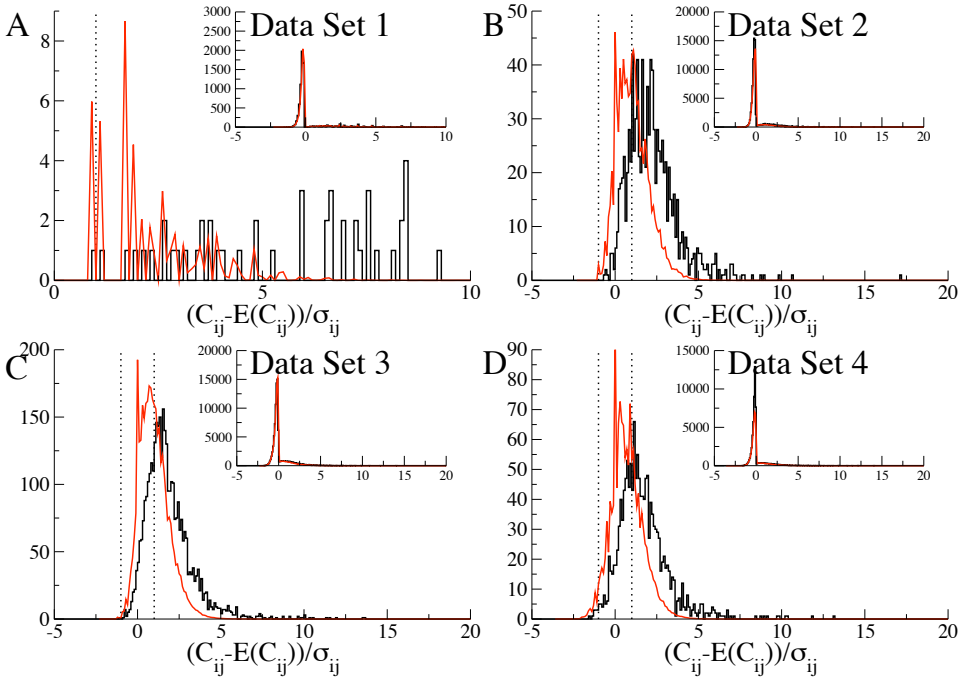

Fig. S.3: Distributions of the pairwise normalized numbers of coincidences for data sets 1-4. A. Data set 1. B. Data set 2. C. Data set 3. D. Data set 4. The insets show the full distributions while the main figures show the distributions after removing all $C_{ij} \leq 2$. Black solid lines: true distributions. Red: prediction assuming Poisson neurons. Dotted black lines: ± 1 standard deviation. See text for details.

0 and 1. The observed values of C_{ij} are, of course, discrete and, in particular, if $C_{ij} = 0$ then this gives a slightly negative contribution. This peak is therefore an artifact of having very short data sets given the low rates. We want to eliminate this artifact by removing all pairs for which C_{ij} is too small. We choose the criterion of $C_{ij} \leq 2$. Doing so leads to the distributions shown in the main panels of Fig.S.3. Now we see that the true distributions and those generated by Poisson neurons are clearly different, with the true one being shifted to the right with respect to the one assuming Poisson neurons. This indicates that there is a significant subset of pairs, with $C_{ij} > 2$, for which the observed number of coincidences cannot be explained by the Poisson hypothesis. Note additionally that for data sets 2-4 the negative tail of the actual distributions lies within that of the Poisson distributions, indicating that whenever the count of C_{ij} is less than predicted, it can be explained just by random fluctuations in a Poisson model, i.e. there is no inhibitory effect. One standard deviation is indicated in Fig.S.3 A-D by a dotted line and is our threshold for assuming non-zero connections, see Eq.2 in the methods section.

Finally, we can ask if including the pairwise interactions p_{ij}, calculated according to Eq.2 in the methods section, can account for the deviation of the true distributions of C_{ij}s with respect to the network of Poisson neurons. Fig.S.4 shows the true distribution for data set 2 (in black) and the distribution of C_{ij}s from a single simulation of the best fit model, model IV of data set 2 (in red). The agreement is good.

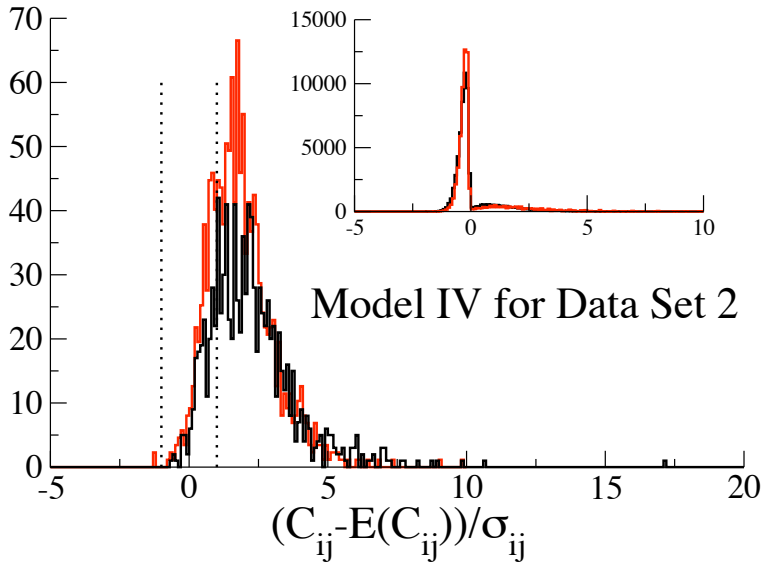

Fig. S.4: The distributions of the pairwise normalized numbers of coincidences from a numerical simulation of model IV fit (in red) to data set 2 (actual data in black).

3 Analyzing a subset of a large data set

The data sets given by the solid red, green and blue circles contain both more neurons and more transitions per neuron than the others. To investigate to what extent these factors influence the poorness of the fit to the Poisson model we subdivided each of the three data sets into smaller data sets. This resulted in a total of ten subsets: 2 for the red circle and 4 for both the green and blue circles. Fig.S.5 shows a summary of the goodness of fit of the non-stationary Poisson model to both the original three data sets as well as each of the subsets, designated by a letter (in all cases the stationary Poisson model gave a worse fit). Of the ten subsets, seven of them yield average goodness-of-fits $\langle d \rangle < 10$.

Details of the goodness-of-fit as a function of jitter are given in Figs.S.6-S.8 for the red, green and blue data sets respectively. In each case the goodness-of-fit as a function of the jitter, $d(J)$, is shown for the original data set (solid line) as well as each subset (dotted lines). The inset shows a scatter plot of the number of transitions per neuron vs the number of neurons in each of the original 15 data sets (crosses and solid colored circle) as well as for the

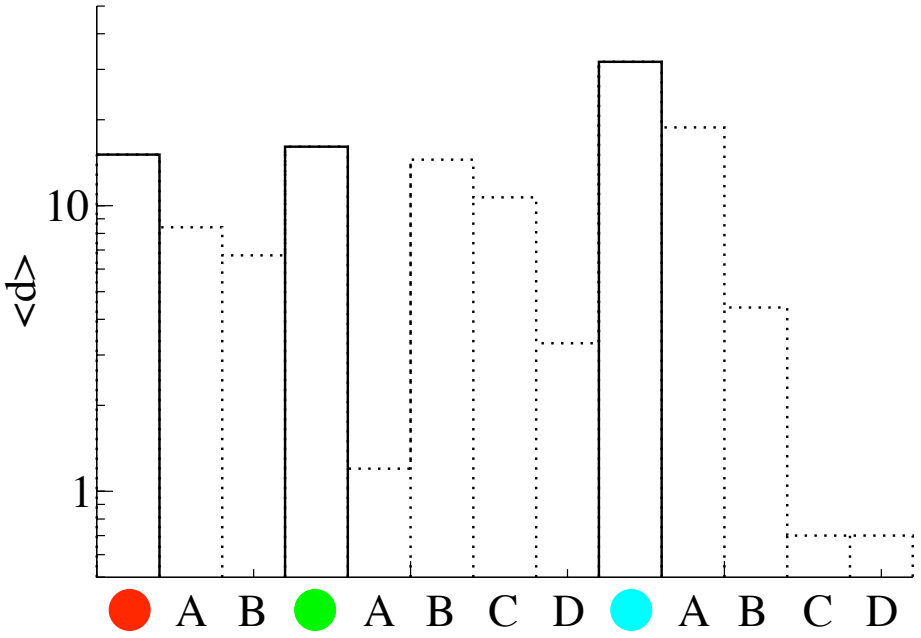

Fig. S.5: Average goodness-of-fit for the nonstationary Poisson model for the three original data sets (solid bars and symbols) and the subsets (dotted bars and letters) resulting from dividing the original data sets into pieces. Seven of the subsets give an order 1 fit.

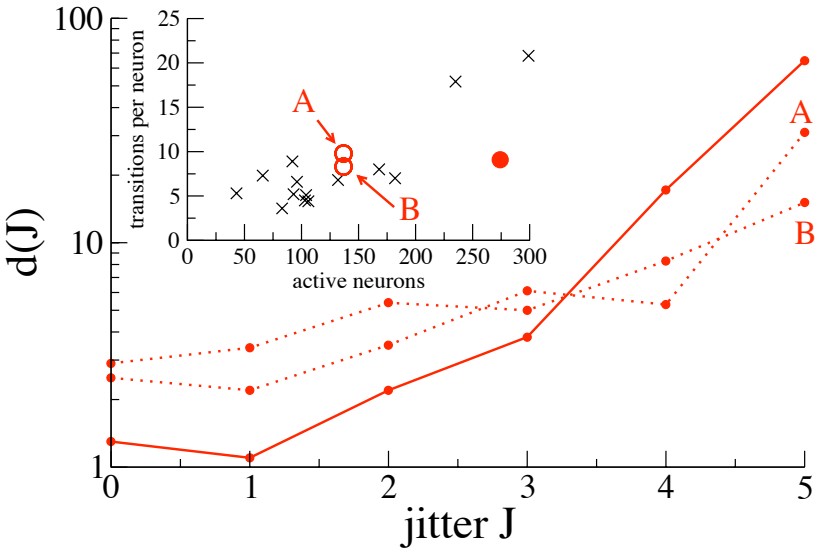

Fig. S.6: The goodness-of-fit as a function of jitter for the nonstationary Poisson model for the data set given by the solid red circle (solid line) and each subset (dotted lines). Inset: The number of transitions per neuron vs the number of active neurons in each of the 15 original data sets (crosses and solid circle) and the two subsets (open circles).

subsets.

These results suggest that the 10 smaller data sets which were best fit by a Poisson model may, in fact, have required a model with interactions had the data sets been larger.

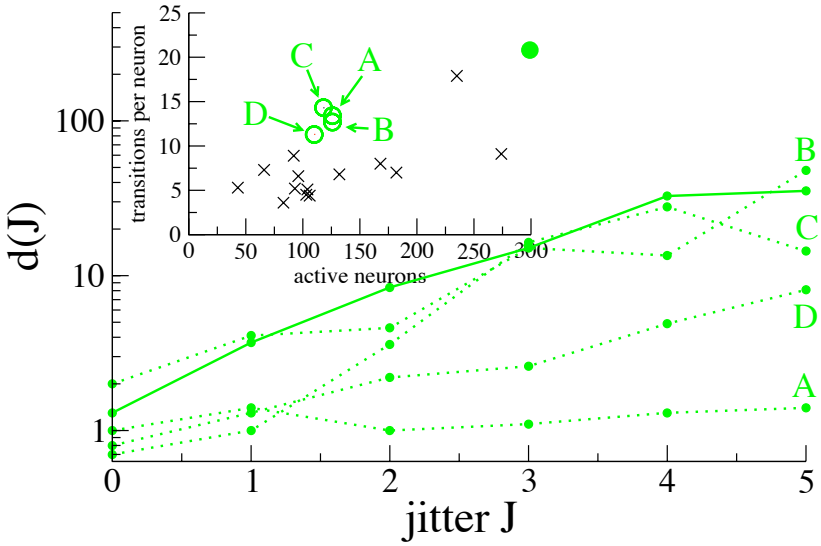

Fig. S.7: The goodness-of-fit as a function of jitter for the nonstationary Poisson model for the data set given by the solid green circle (solid line) and each subset (dotted lines). Inset: The number of transitions per neuron vs the number of active neurons in each of the 15 original data sets (crosses and solid circle) and the four subsets (open circles).

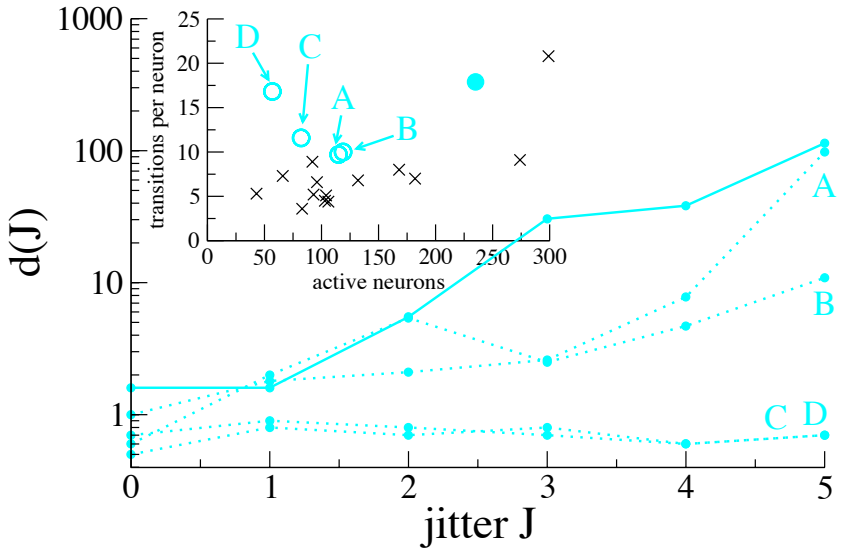

Fig. S.8: The goodness-of-fit as a function of jitter for the nonstationary Poisson model for the data set given by the solid blue circle (solid line) and each subset (dotted lines). Inset: The number of transitions per neuron vs the number of active neurons in each of the 15 original data sets (crosses and solid circle) and the four subsets (open circles).

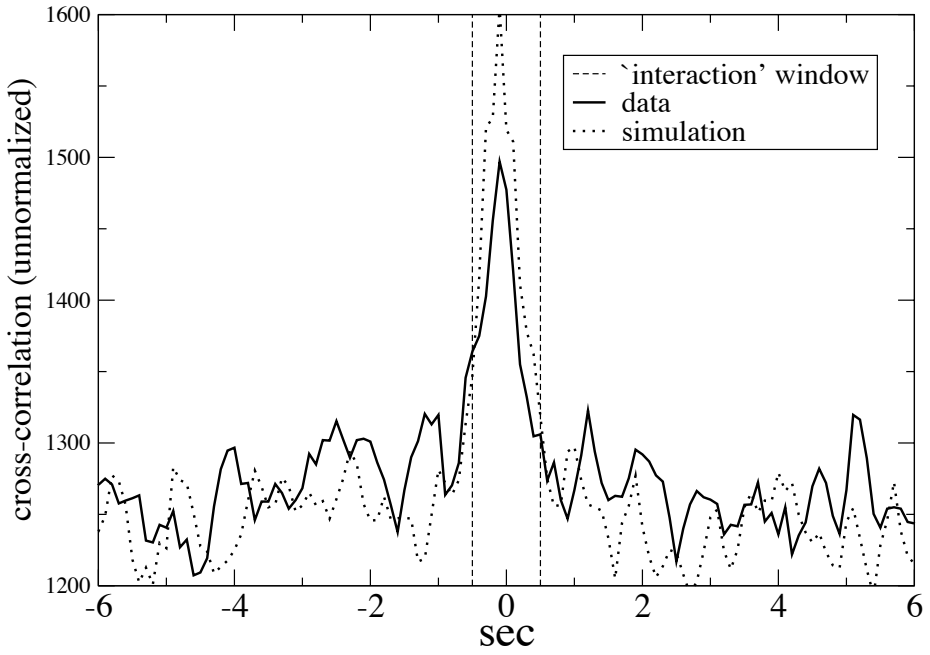

Fig. S.9: Cross-correlation of data from data set given by the solid blue circle (solid line), and simulated data using the model with interactions (dotted line). The cross-correlograms are not normalized. The dashed lines indicate the range of interactions in the model (±500ms). Both curves are smoothed with a running average of two bins (200ms).

4 The distribution of delays in the models with interactions.

We chose a uniform distribution in the delays as it is the weakest assumption we can make given our lack of knowledge concerning the true distribution. As a check of the validity of this choice, we calculate the cross-correlogram of the transitions for all pairs of neurons in data set 4 (blue solid circle) and compare this to a cross-correlogram of simulated transitions from model 4 (nonstationary model with interactions). This comparison is shown in Fig.S.9 and indicates good qualitative agreement. Note that interactions are present only between a small fraction of pairs (4.5% of pairs for data set 4) while the cross-correlogram in Fig.S.9 is for all pairs.

In order to test the robustness of the choice of a uniform distribution in

delays, we also fit models 3 and 4 to data sets 1-4 using a distribution in the delay which decayed in time. Specifically, we have done simulations in which the latency of interactions follows a probability distribution with a delay of one frame with p = 0.5, two frames with p = 0.2 and three, four or five frames with p = 0.1 each. This distribution is thus sharply decaying in time. The goodness-of-fit measure $\langle d \rangle$ averaged over all values of the jitter for 100 simulations for data sets 1-4 (those with significant pairwise interactions) using this distribution is 2.5, 2.6, 2.2 and 8.3 respectively compared to 3.9, 4.1, 2.8 and 6.1 with the uniform distribution. These values are of the same order for both types of distributions, suggesting that the time-scale of interactions (100s of ms) is the most crucial aspect of the distribution and not the exact shape.

5 Raw data and pattern distributions

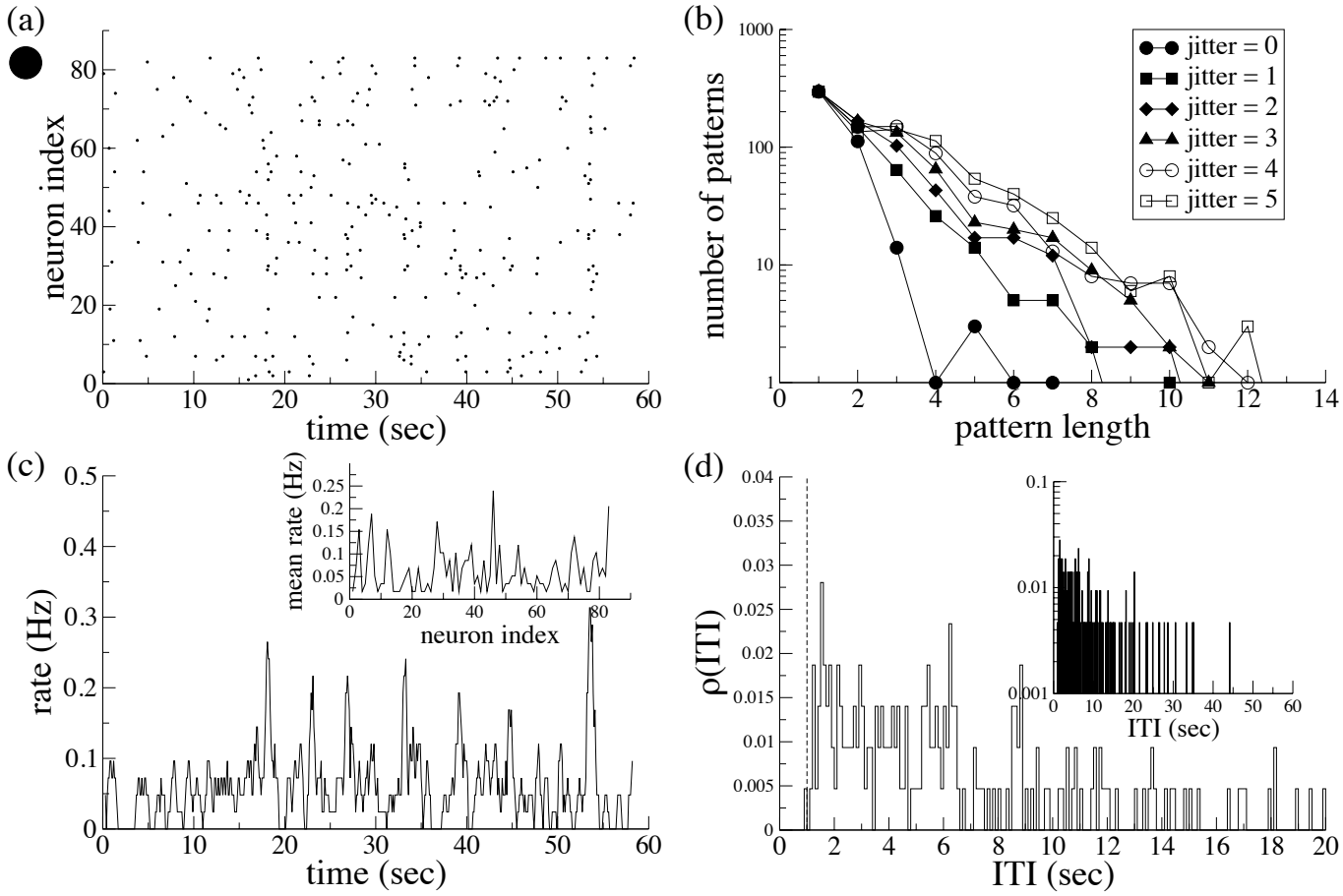

Fig. S.10: Equivalent of Fig.1 from main text for data set given by symbol in panel (a). (a) Raster. (b) Pattern distributions. (c) Transition rate. Inset: rate of each neuron. (d) Inter-transition interval (ITI). Effective refractory period used in model shown by dashed line.

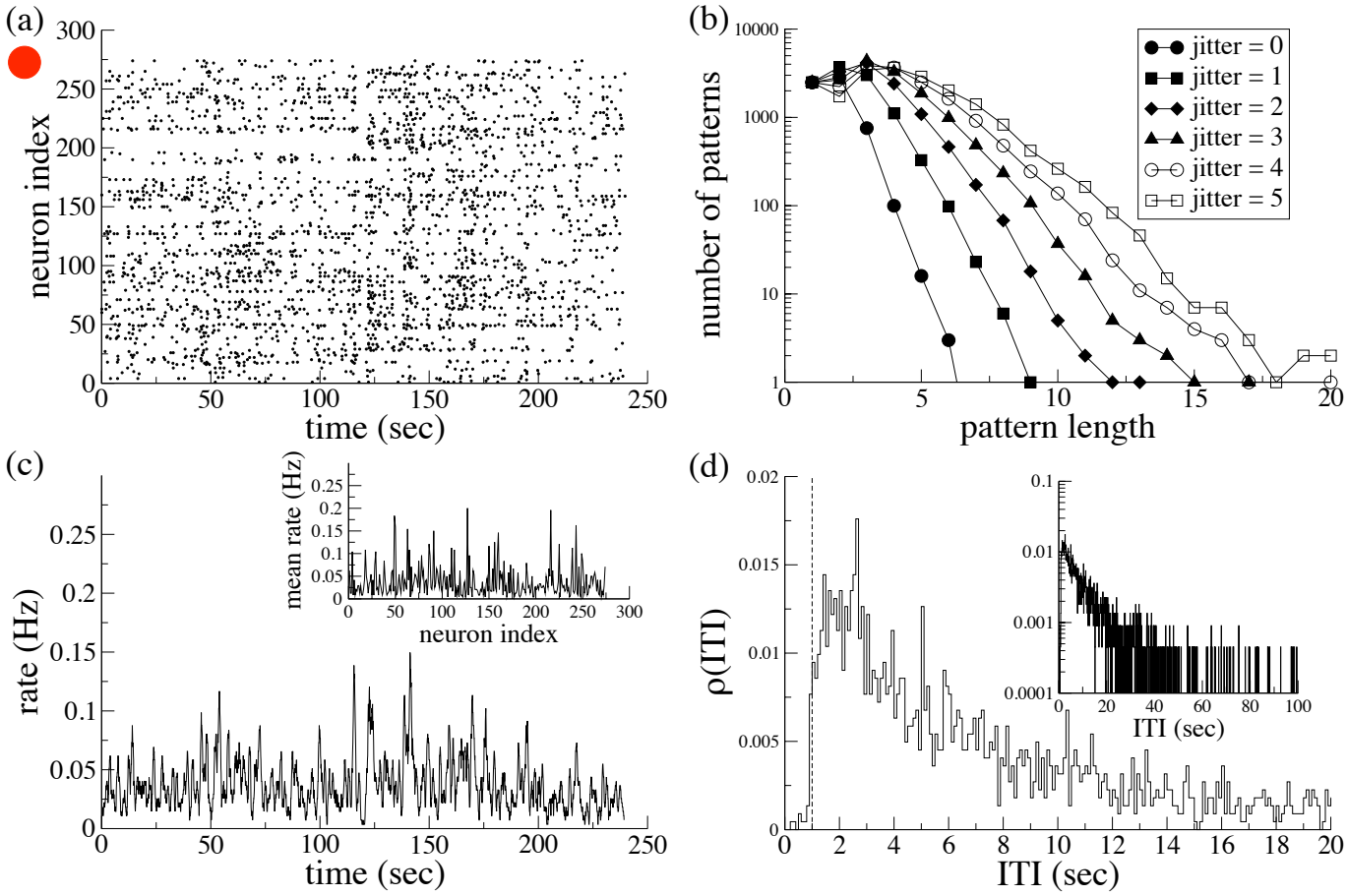

Fig. S.11: Equivalent of Fig.1 from main text for data set given by symbol in panel (a). (a) Raster. (b) Pattern distributions. (c) Transition rate. Inset: rate of each neuron. (d) Inter-transition interval (ITI). Effective refractory period used in model shown by dashed line.

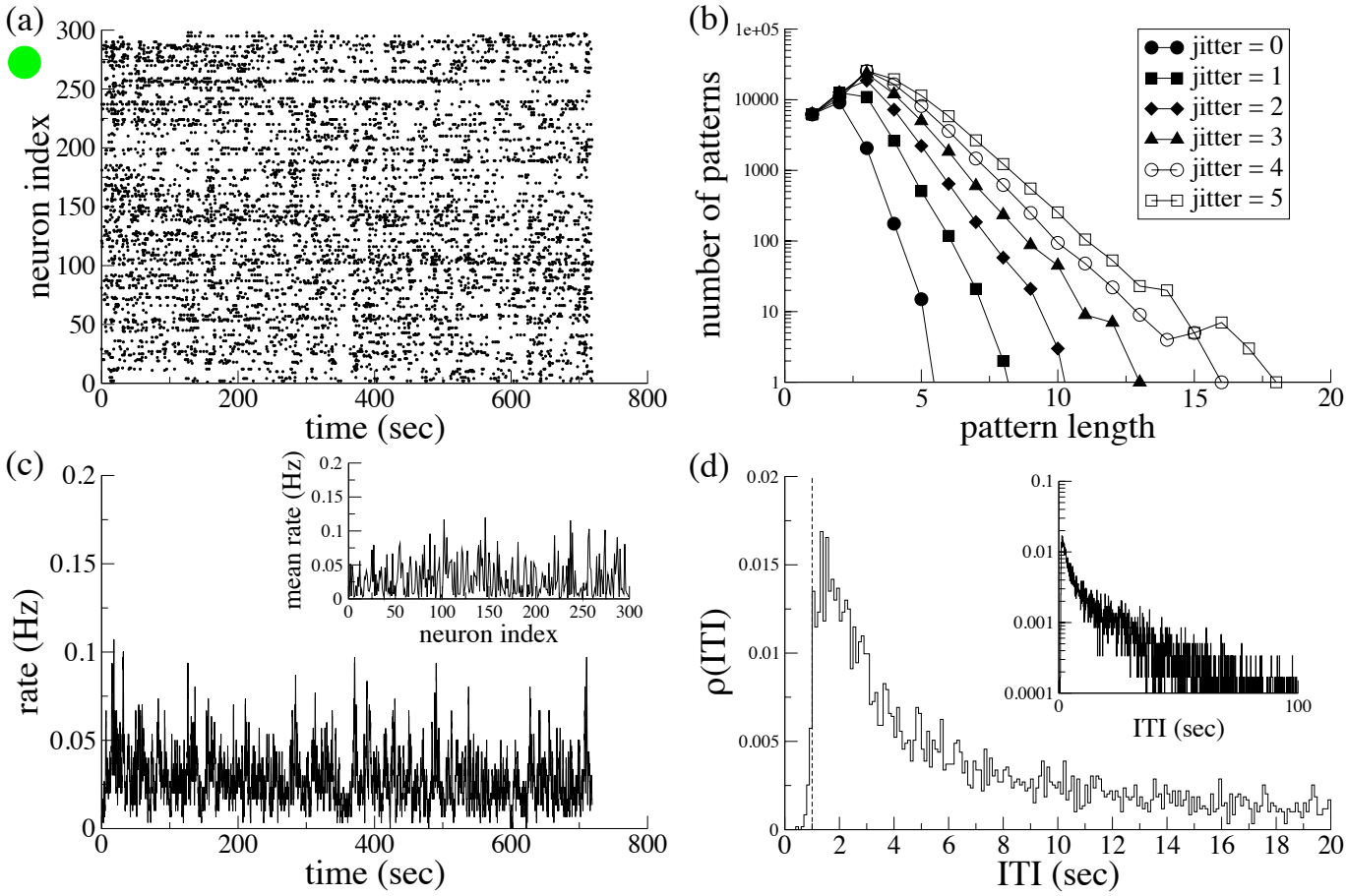

Fig. S.12: Equivalent of Fig.1 from main text for data set given by symbol in panel (a). (a) Raster. (b) Pattern distributions. (c) Transition rate. Inset: rate of each neuron. (d) Inter-transition interval (ITI). Effective refractory period used in model shown by dashed line.

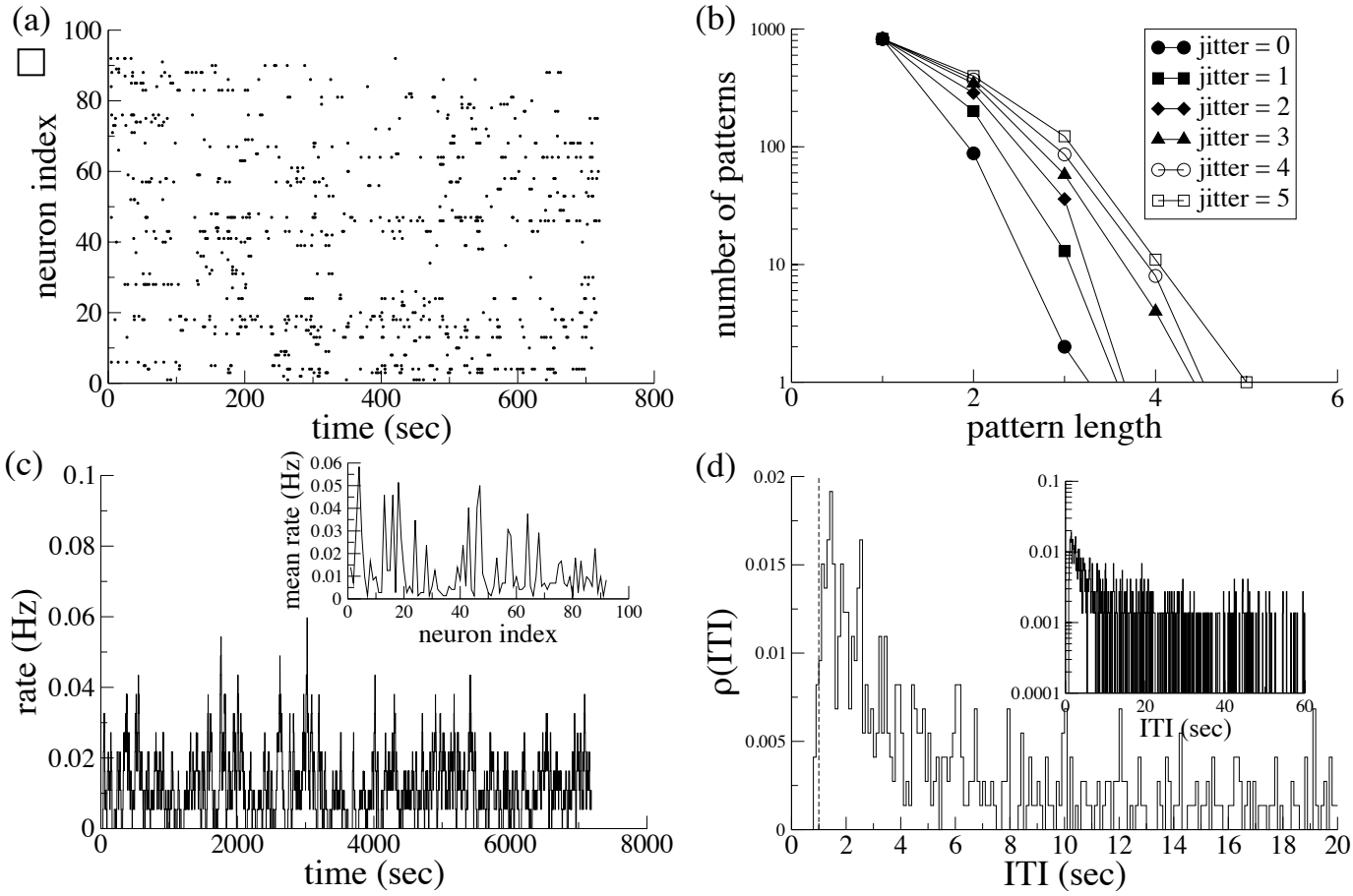

Fig. S.13: Equivalent of Fig.1 from main text for data set given by symbol in panel (a). (a) Raster. (b) Pattern distributions. (c) Transition rate. Inset: rate of each neuron. (d) Inter-transition interval (ITI). Effective refractory period used in model shown by dashed line.

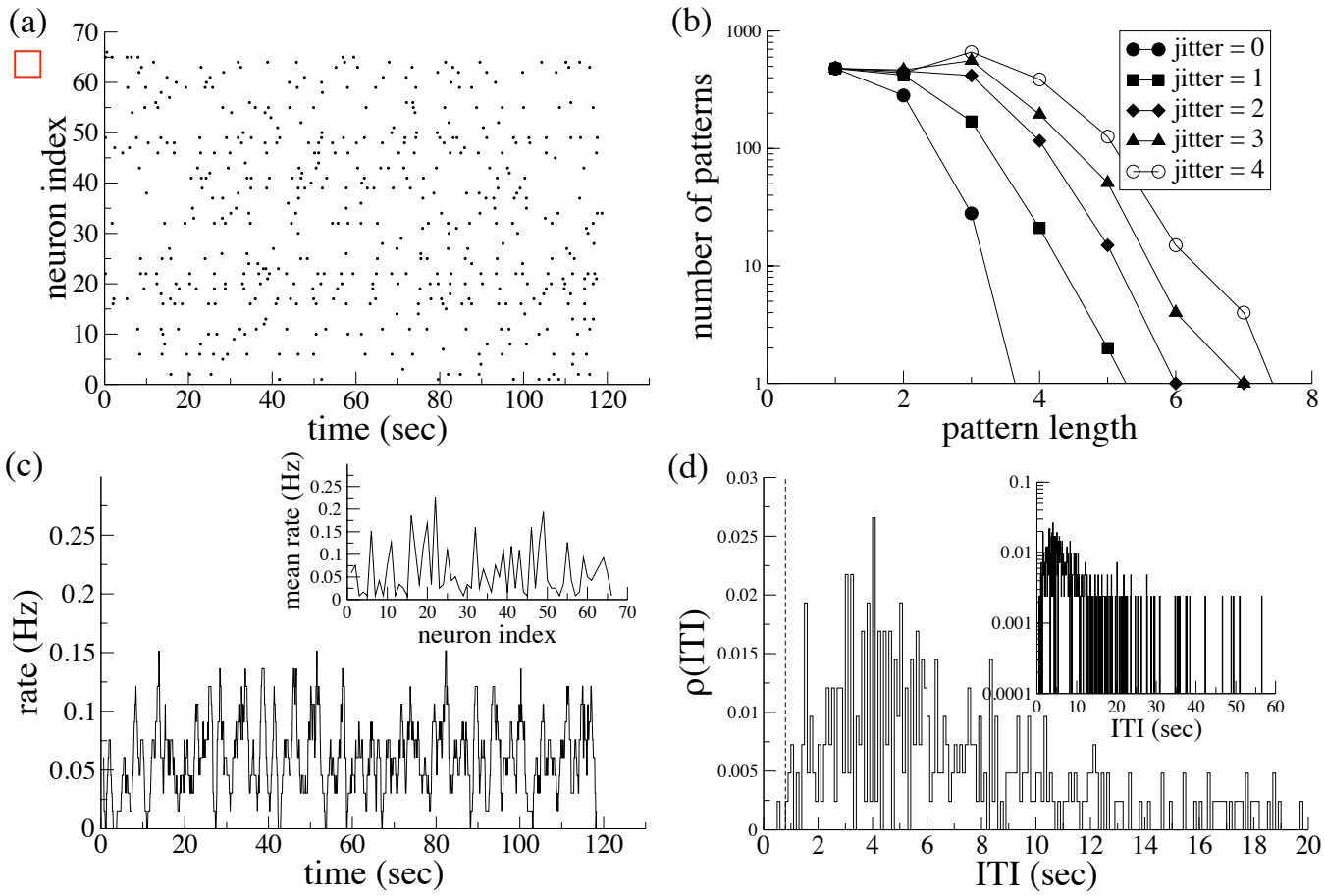

Fig. S.14: Equivalent of Fig.1 from main text for data set given by symbol in panel (a). (a) Raster. (b) Pattern distributions. (c) Transition rate. Inset: rate of each neuron. (d) Inter-transition interval (ITI). Effective refractory period used in model shown by dashed line.

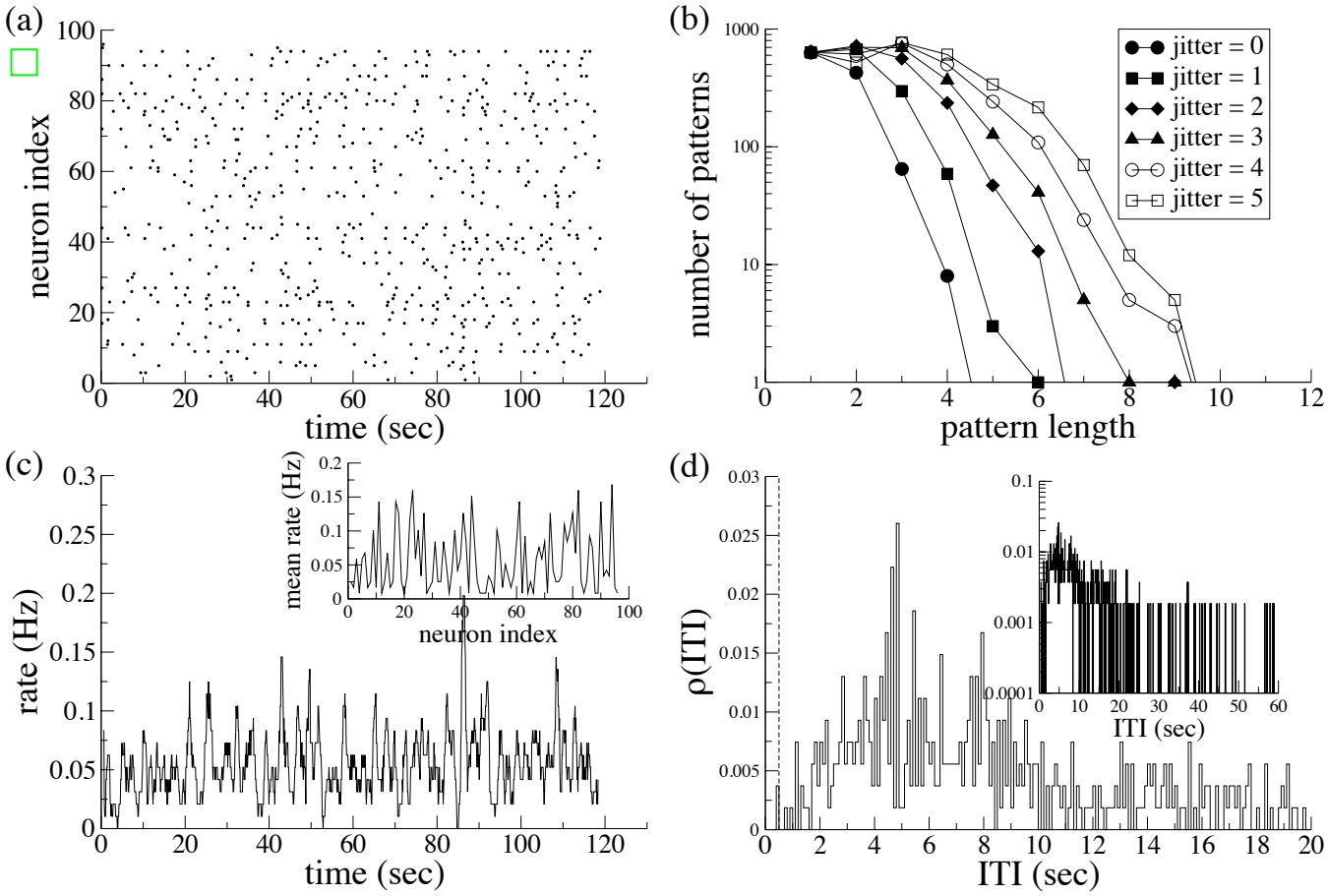

Fig. S.15: Equivalent of Fig.1 from main text for data set given by symbol in panel (a). (a) Raster. (b) Pattern distributions. (c) Transition rate. Inset: rate of each neuron. (d) Inter-transition interval (ITI). Effective refractory period used in model shown by dashed line.

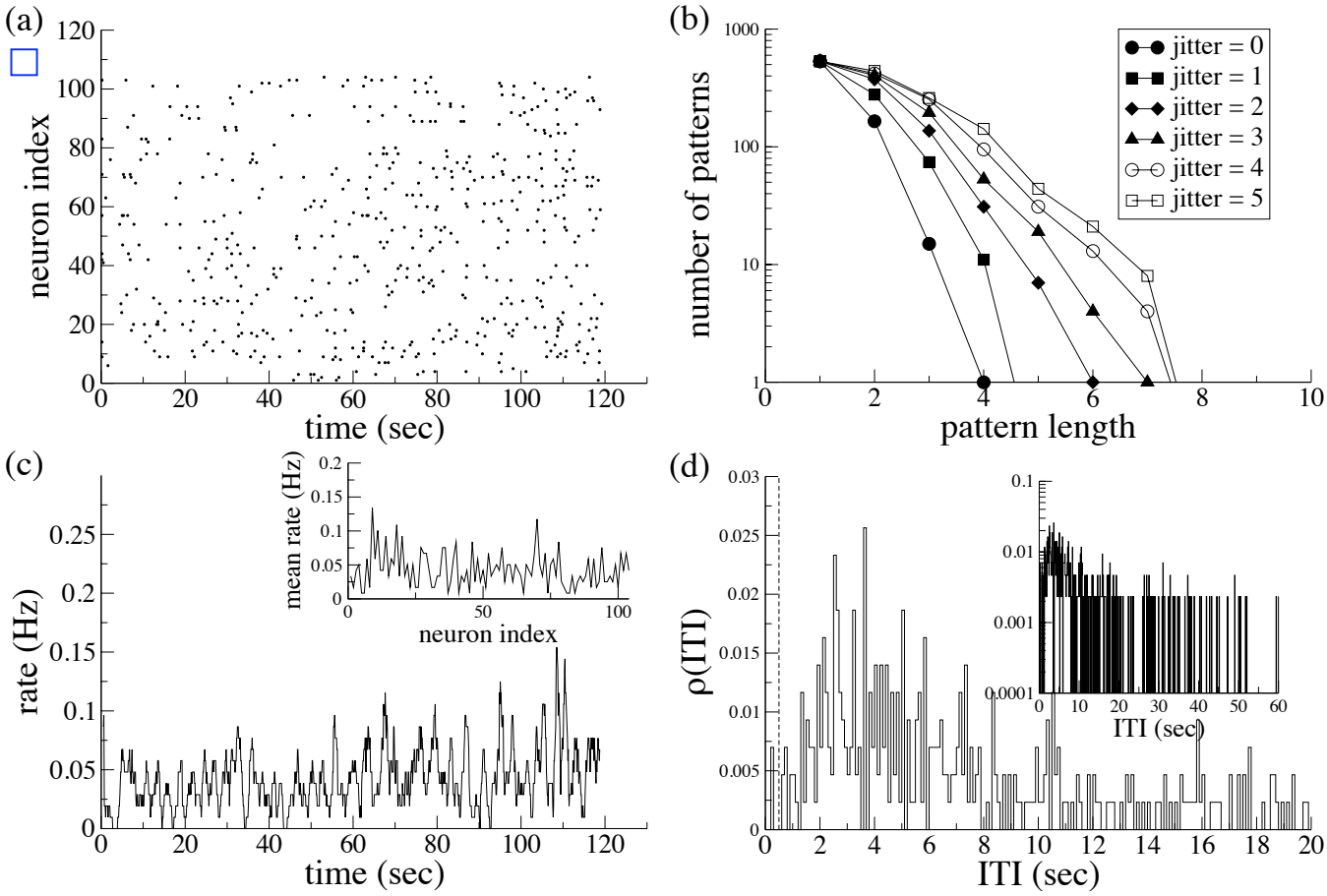

Fig. S.16: Equivalent of Fig.1 from main text for data set given by symbol in panel (a). (a) Raster. (b) Pattern distributions. (c) Transition rate. Inset: rate of each neuron. (d) Inter-transition interval (ITI). Effective refractory period used in model shown by dashed line.

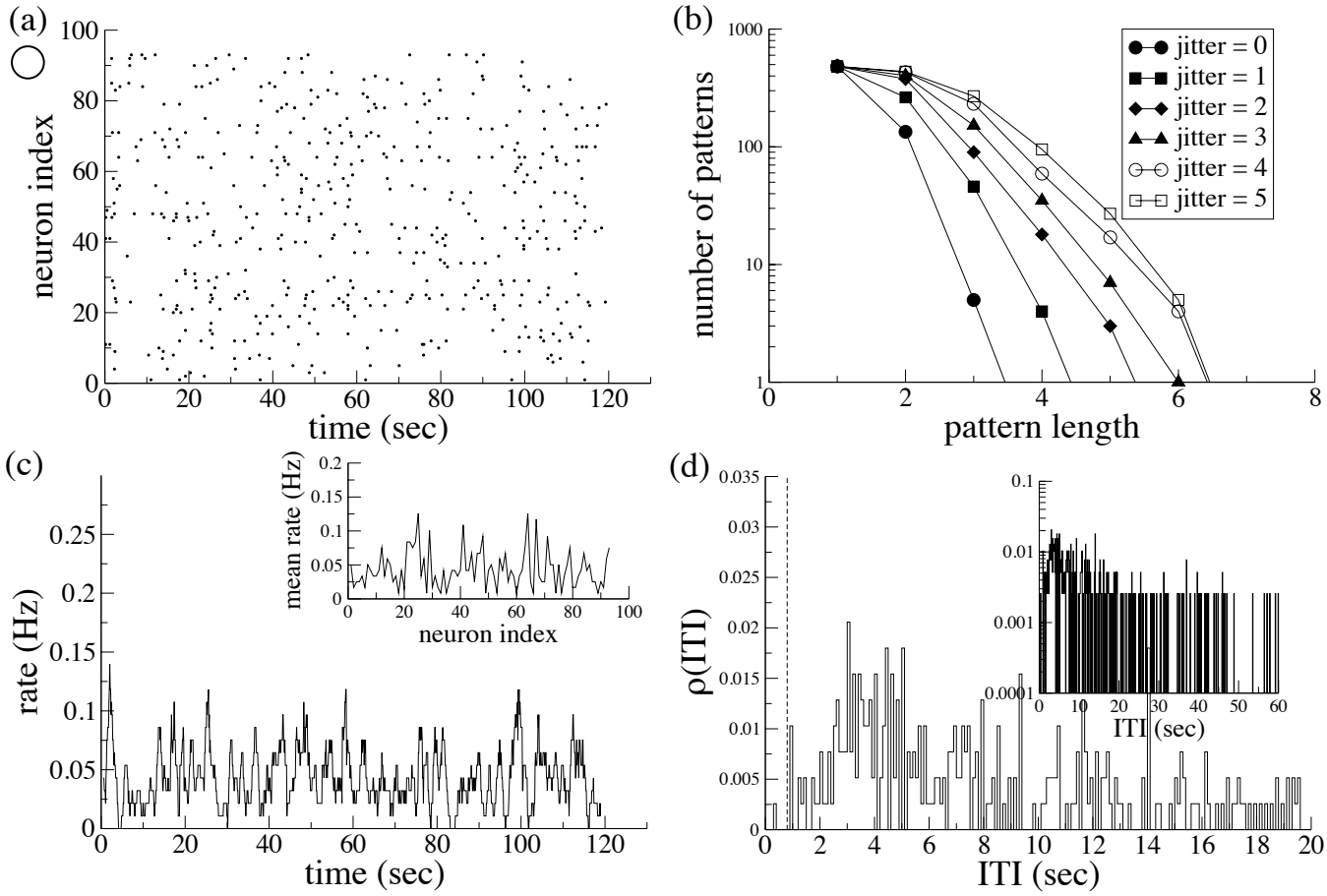

Fig. S.17: Equivalent of Fig.1 from main text for data set given by symbol in panel (a). (a) Raster. (b) Pattern distributions. (c) Transition rate. Inset: rate of each neuron. (d) Inter-transition interval (ITI). Effective refractory period used in model shown by dashed line.

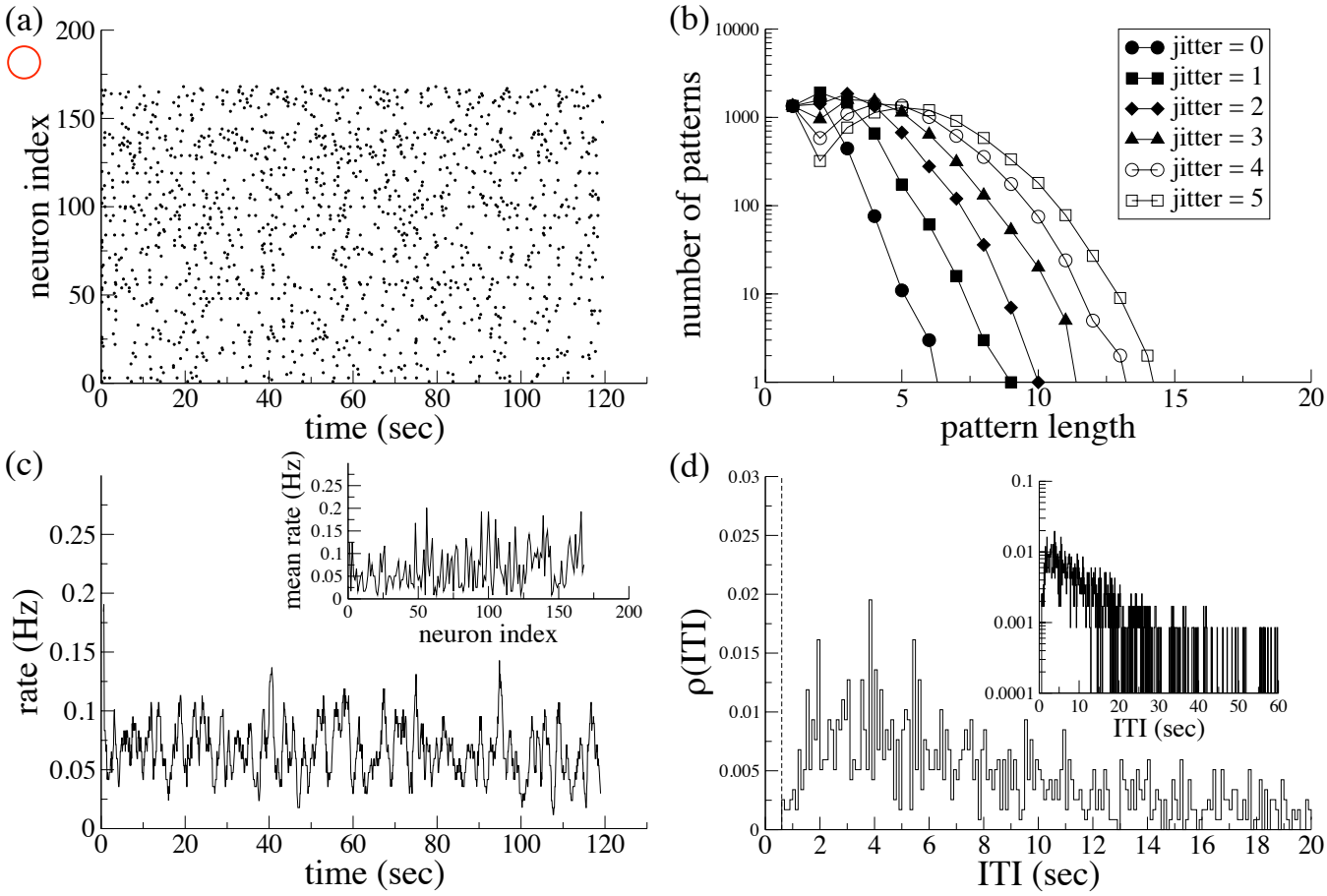

Fig. S.18: Equivalent of Fig.1 from main text for data set given by symbol in panel (a). (a) Raster. (b) Pattern distributions. (c) Transition rate. Inset: rate of each neuron. (d) Inter-transition interval (ITI). Effective refractory period used in model shown by dashed line.

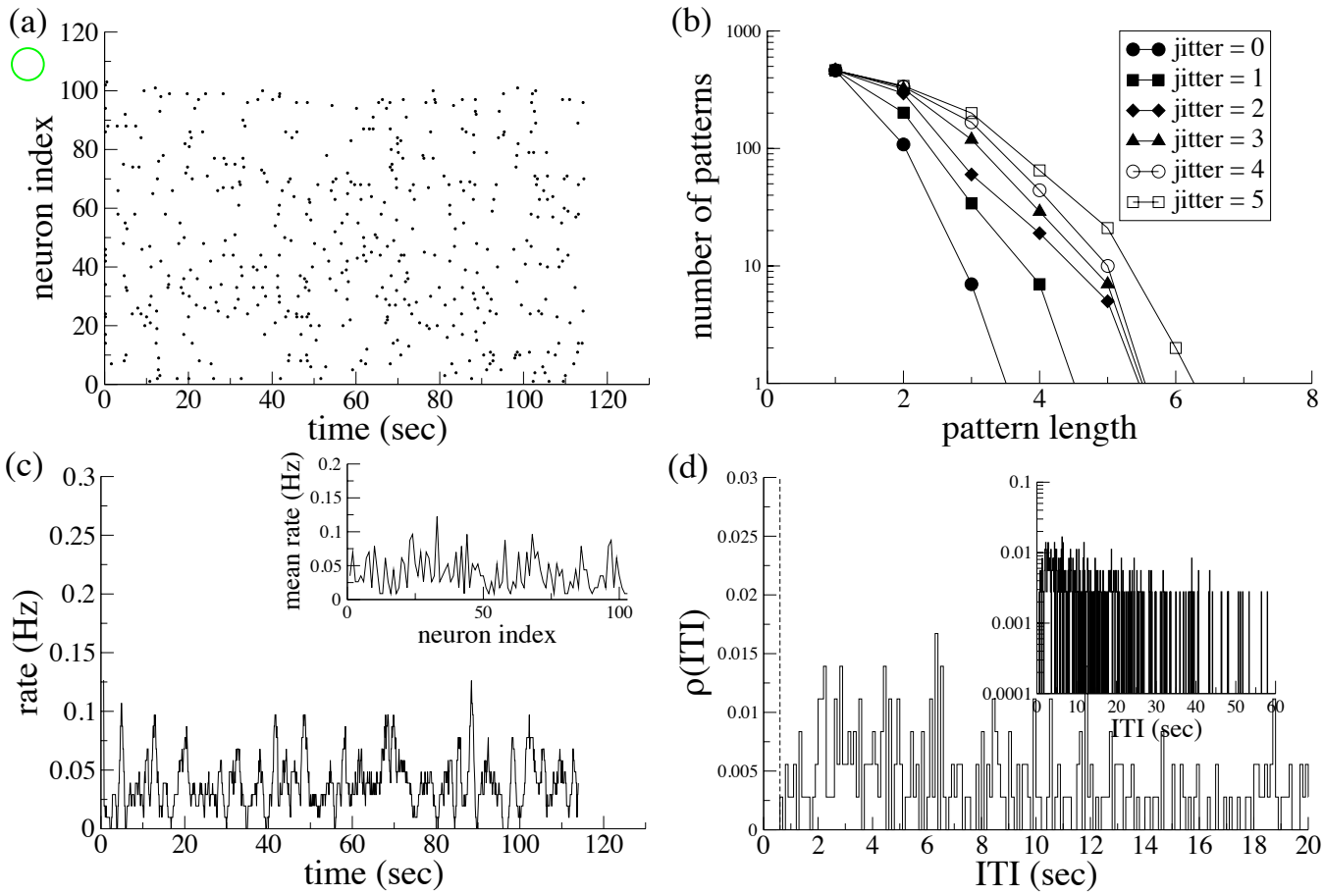

Fig. S.19: Equivalent of Fig.1 from main text for data set given by symbol in panel (a). (a) Raster. (b) Pattern distributions. (c) Transition rate. Inset: rate of each neuron. (d) Inter-transition interval (ITI). Effective refractory period used in model shown by dashed line.

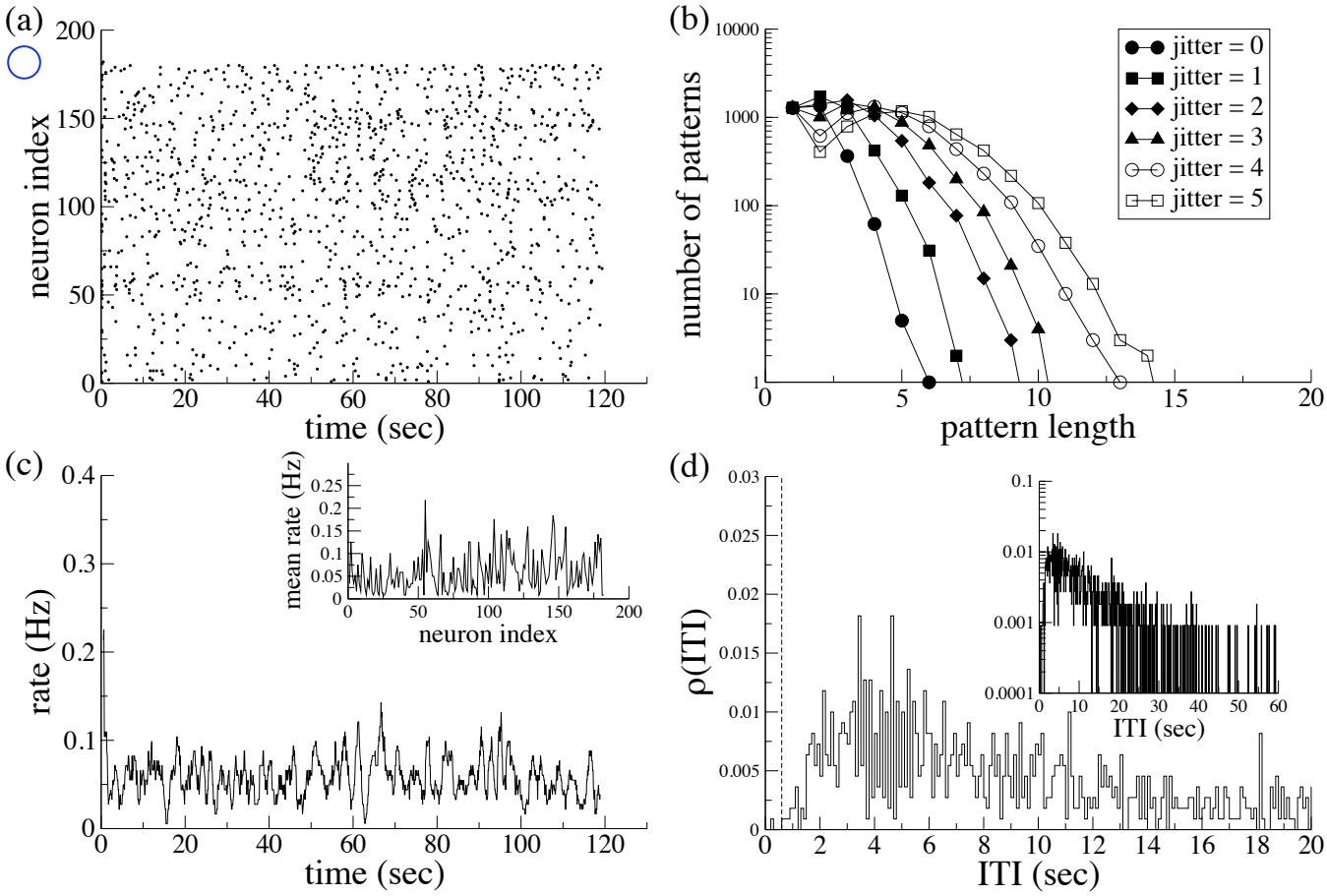

Fig. S.20: Equivalent of Fig.1 from main text for data set given by symbol in panel (a). (a) Raster. (b) Pattern distributions. (c) Transition rate. Inset: rate of each neuron. (d) Inter-transition interval (ITI). Effective refractory period used in model shown by dashed line.

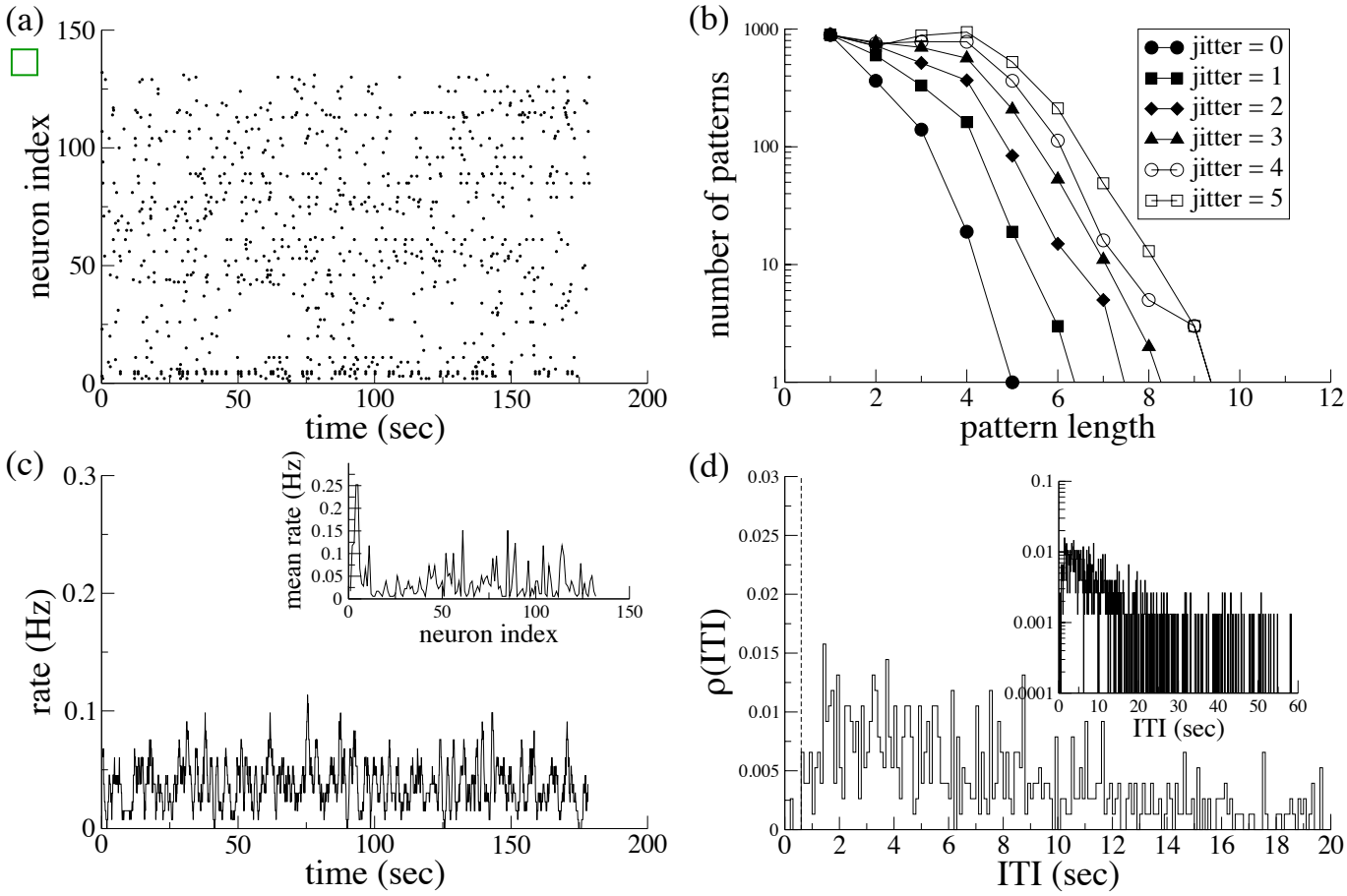

Fig. S.21: Equivalent of Fig.1 from main text for data set given by symbol in panel (a). (a) Raster. (b) Pattern distributions. (c) Transition rate. Inset: rate of each neuron. (d) Inter-transition interval (ITI). Effective refractory period used in model shown by dashed line.

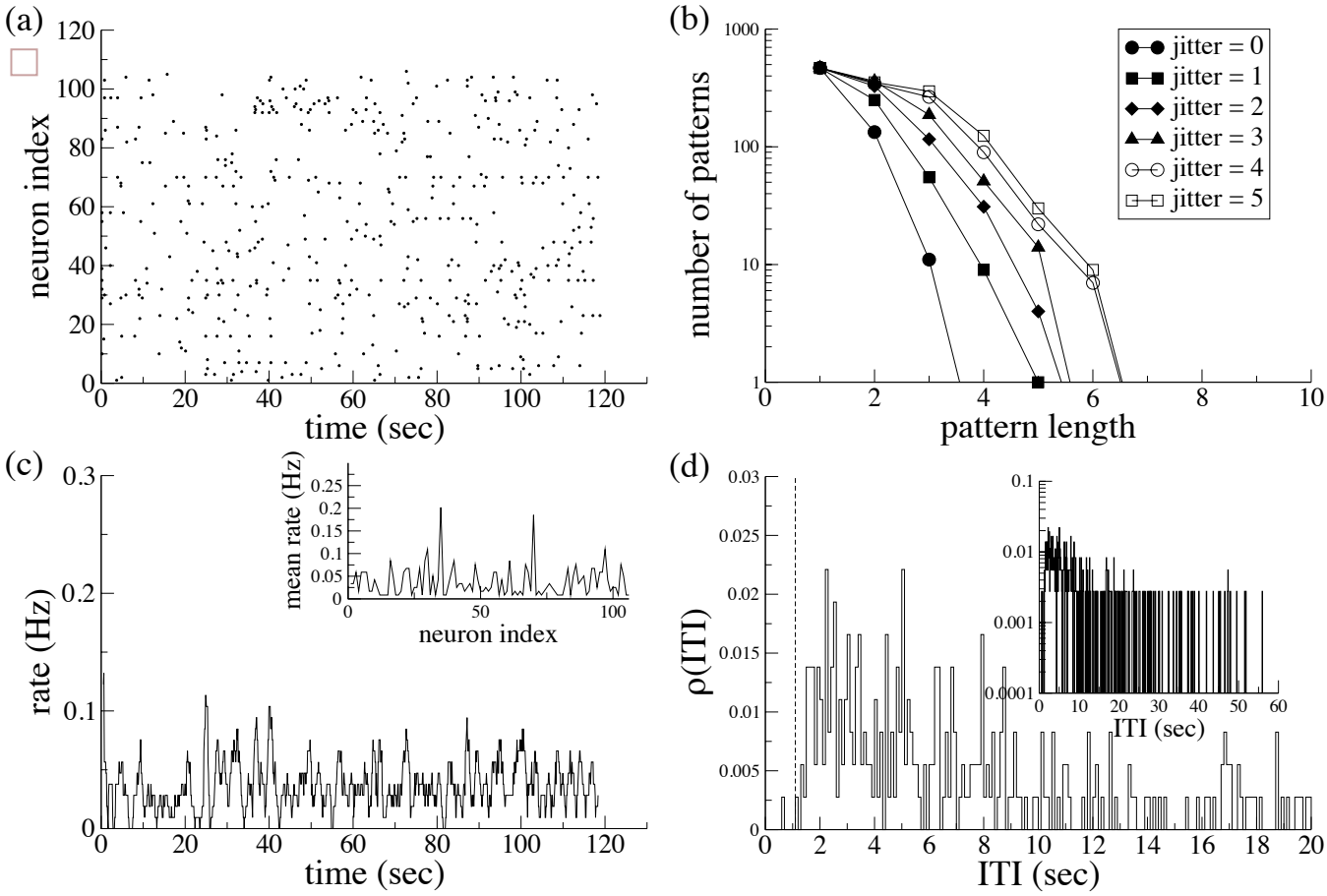

Fig. S.22: Equivalent of Fig.1 from main text for data set given by symbol in panel (a). (a) Raster. (b) Pattern distributions. (c) Transition rate. Inset: rate of each neuron. (d) Inter-transition interval (ITI). Effective refractory period used in model shown by dashed line.

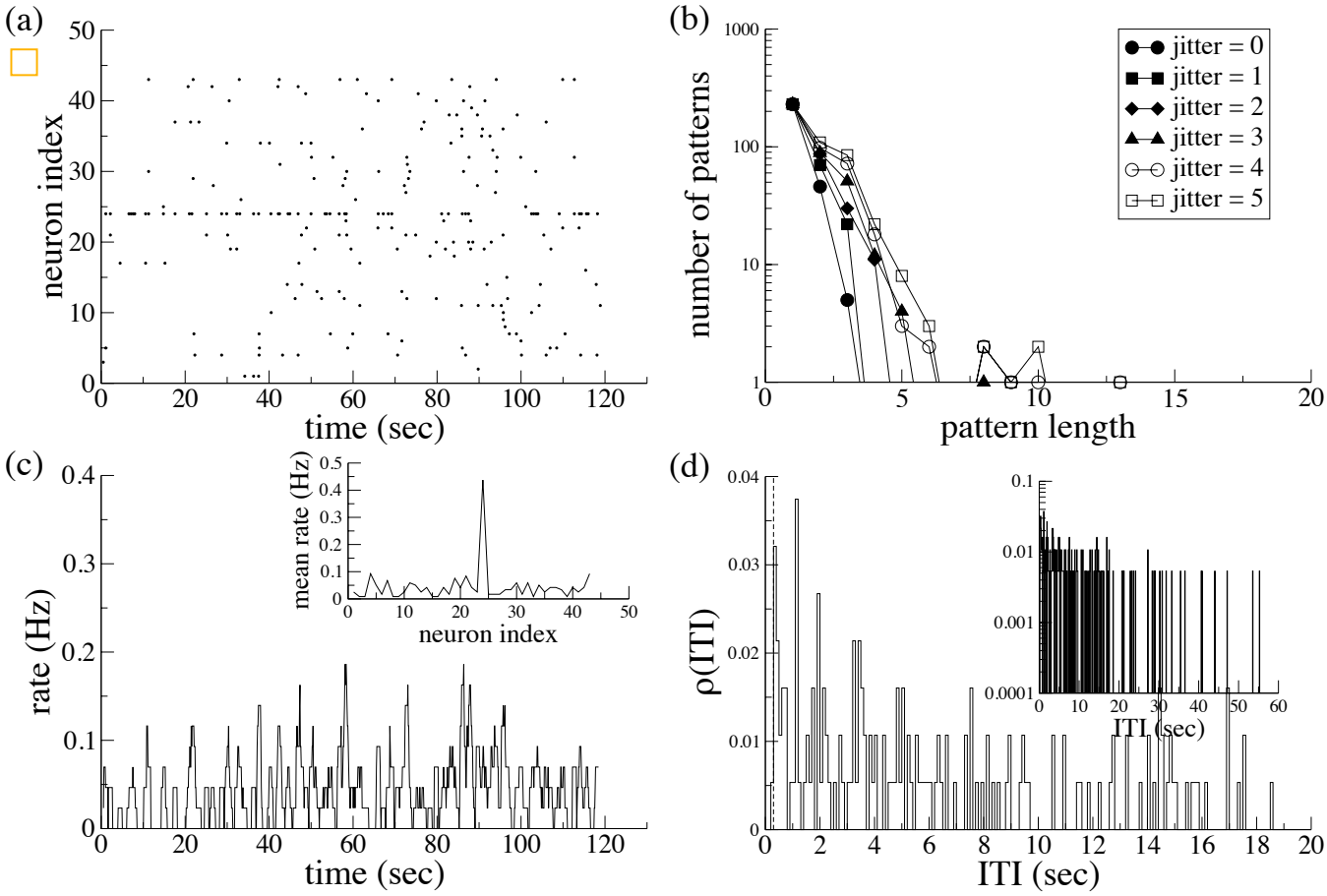

Fig. S.23: Equivalent of Fig.1 from main text for data set given by symbol in panel (a). (a) Raster. (b) Pattern distributions. (c) Transition rate. Inset: rate of each neuron. (d) Inter-transition interval (ITI). Effective refractory period used in model shown by dashed line.

6 Pattern Distributions

6.1 Model 1: Stationary Poisson Model.

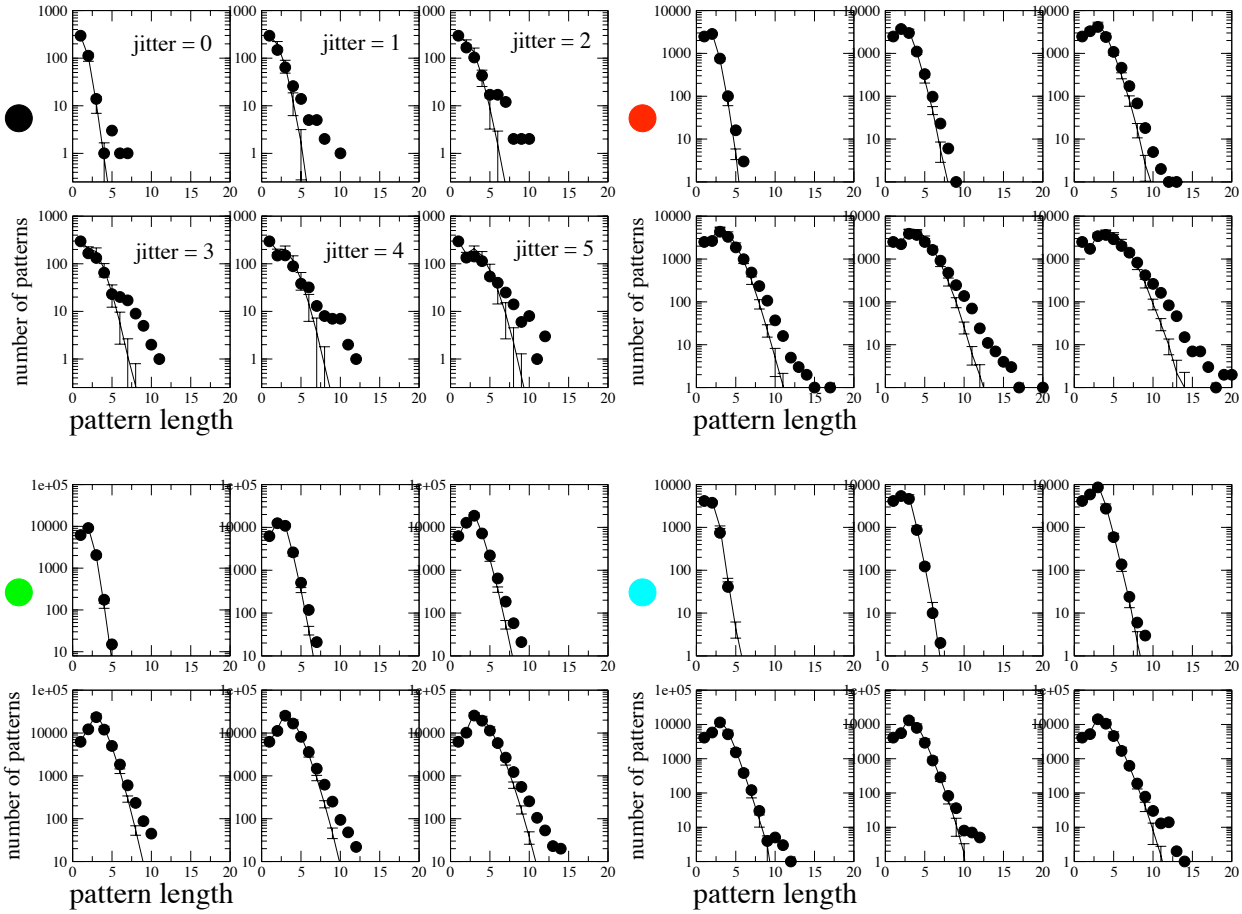

Fig. S.24: Pattern distributions. Circles: from experimental data. The corresponding data set is indicated by the symbol to the left of the figure. Lines: Results from 100 simulations of model 1. Error bars indicate one standard deviation. Shown are distributions for 6 values of the jitter, 0 to 5.

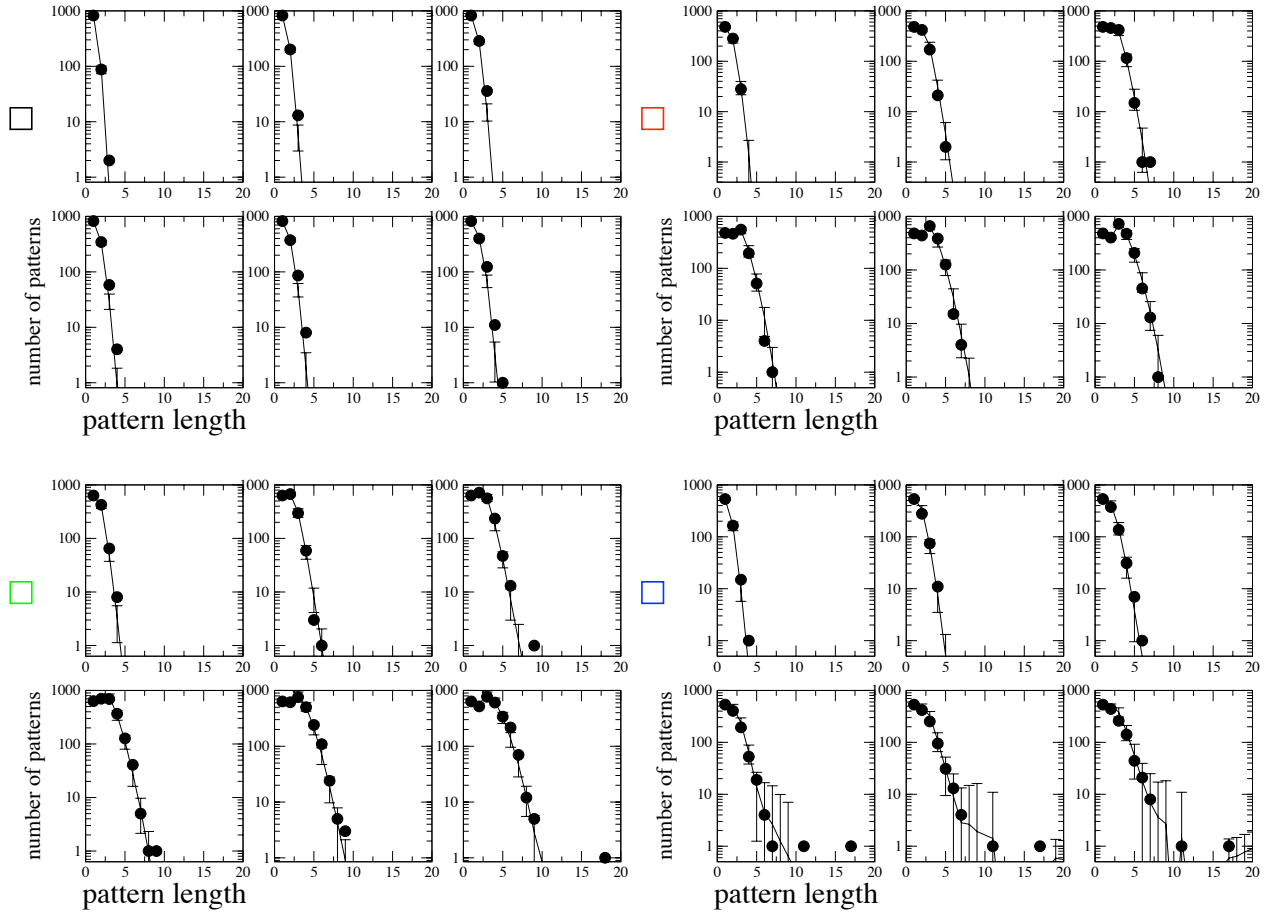

Fig. S.25: Pattern distributions. Circles: from experimental data. The corresponding data set is indicated by the symbol to the left of the figure. Lines: Results from 100 simulations of model 1. Error bars indicate one standard deviation. Shown are distributions for 6 values of the jitter, 0 to 5.

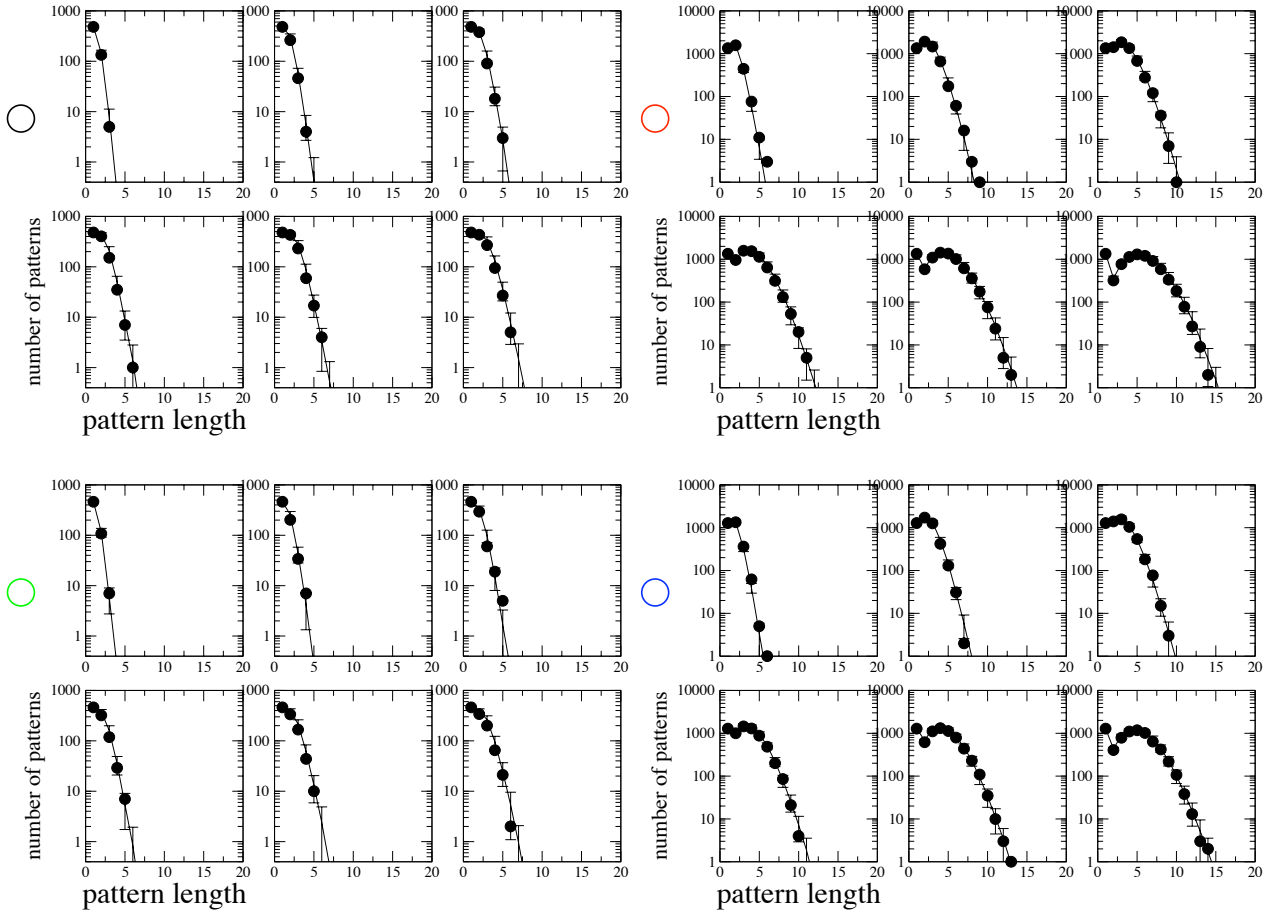

Fig. S.26: Pattern distributions. Circles: from experimental data. The corresponding data set is indicated by the symbol to the left of the figure. Lines: Results from 100 simulations of model 1. Error bars indicate one standard deviation. Shown are distributions for 6 values of the jitter, 0 to 5.

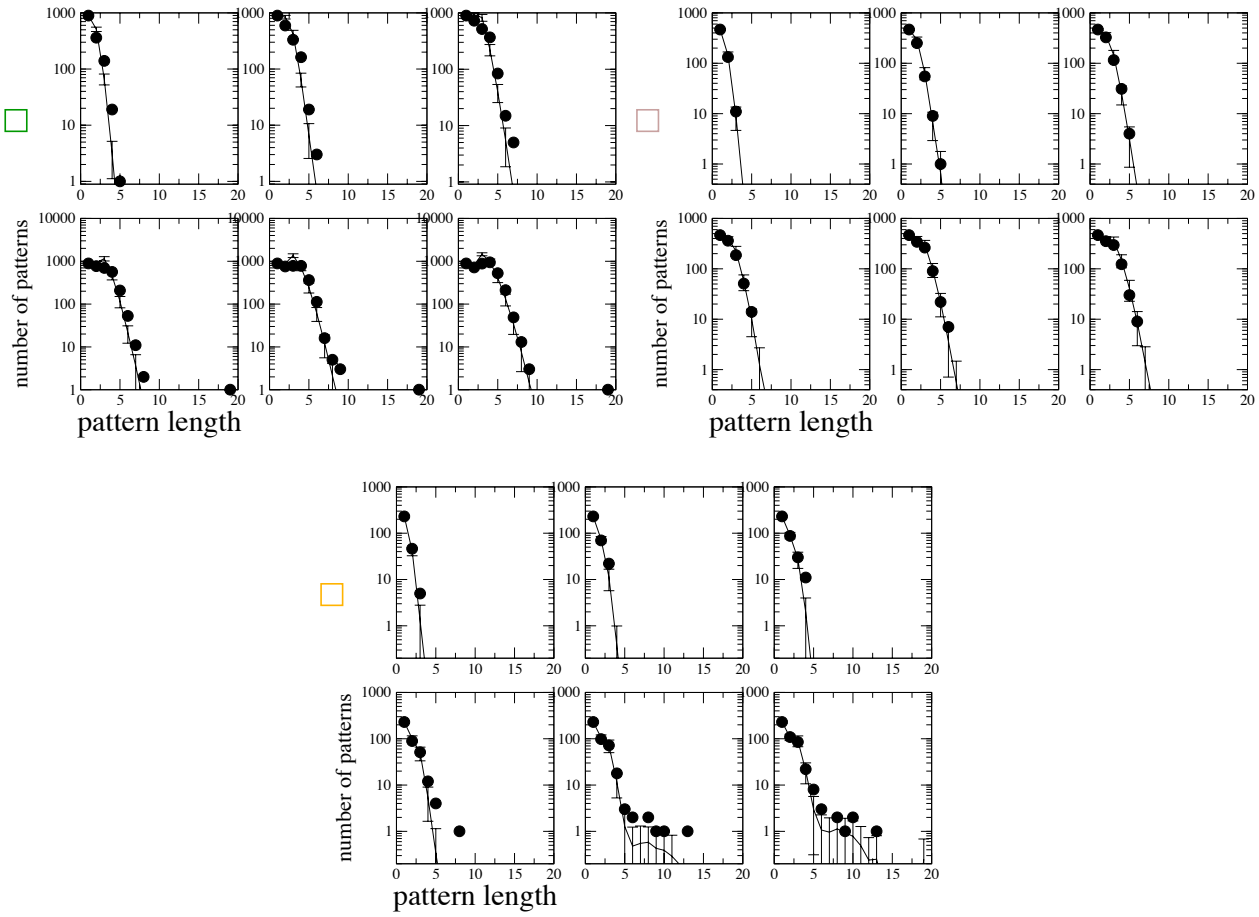

Fig. S.27: Pattern distributions. Circles: from experimental data. The corresponding data set is indicated by the symbol to the left of the figure. Lines: Results from 100 simulations of model 1. Error bars indicate one standard deviation. Shown are distributions for 6 values of the jitter, 0 to 5.

6.2 Model 2: Non-stationary Poisson Model.

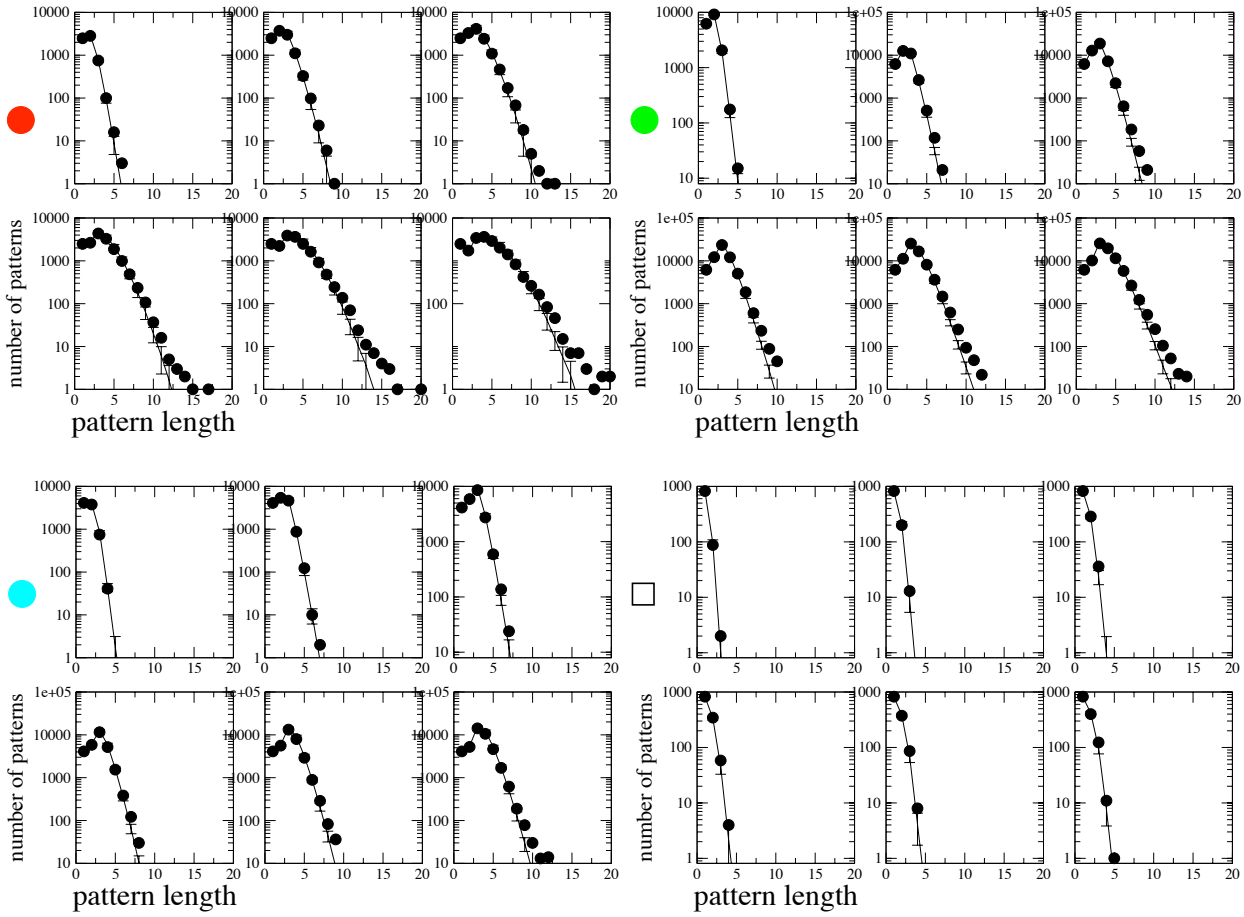

Fig. S.28: Pattern distributions. Circles: from experimental data. The corresponding data set is indicated by the symbol to the left of the figure. Lines: Results from 100 simulations of model 2. Error bars indicate one standard deviation. Shown are distributions for 6 values of the jitter, 0 to 5.

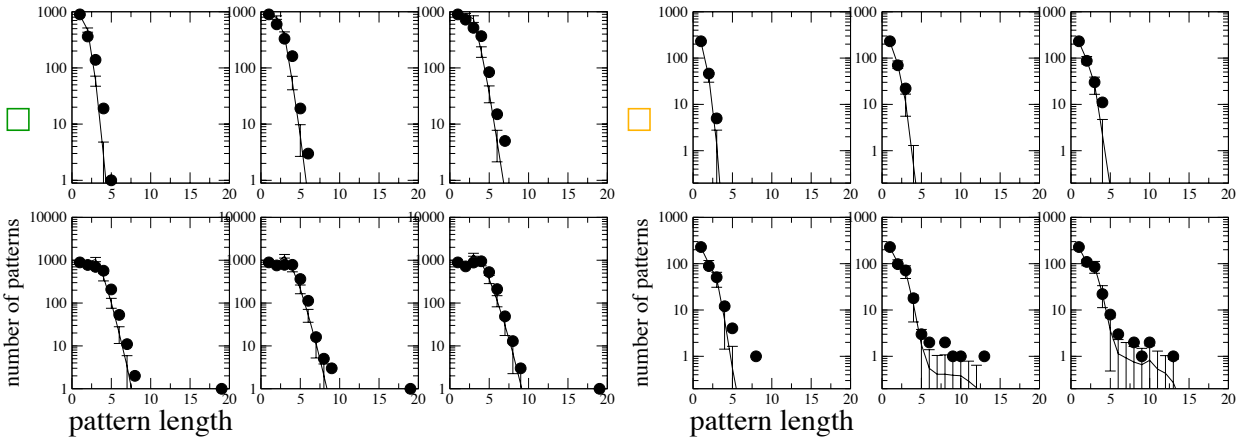

Fig. S.29: Pattern distributions. Circles: from experimental data. The corresponding data set is indicated by the symbol to the left of the figure. Lines: Results from 100 simulations of model 2. Error bars indicate one standard deviation. Shown are distributions for 6 values of the jitter, 0 to 5.

6.3 Model 3: Stationary stochastic model with interactions.

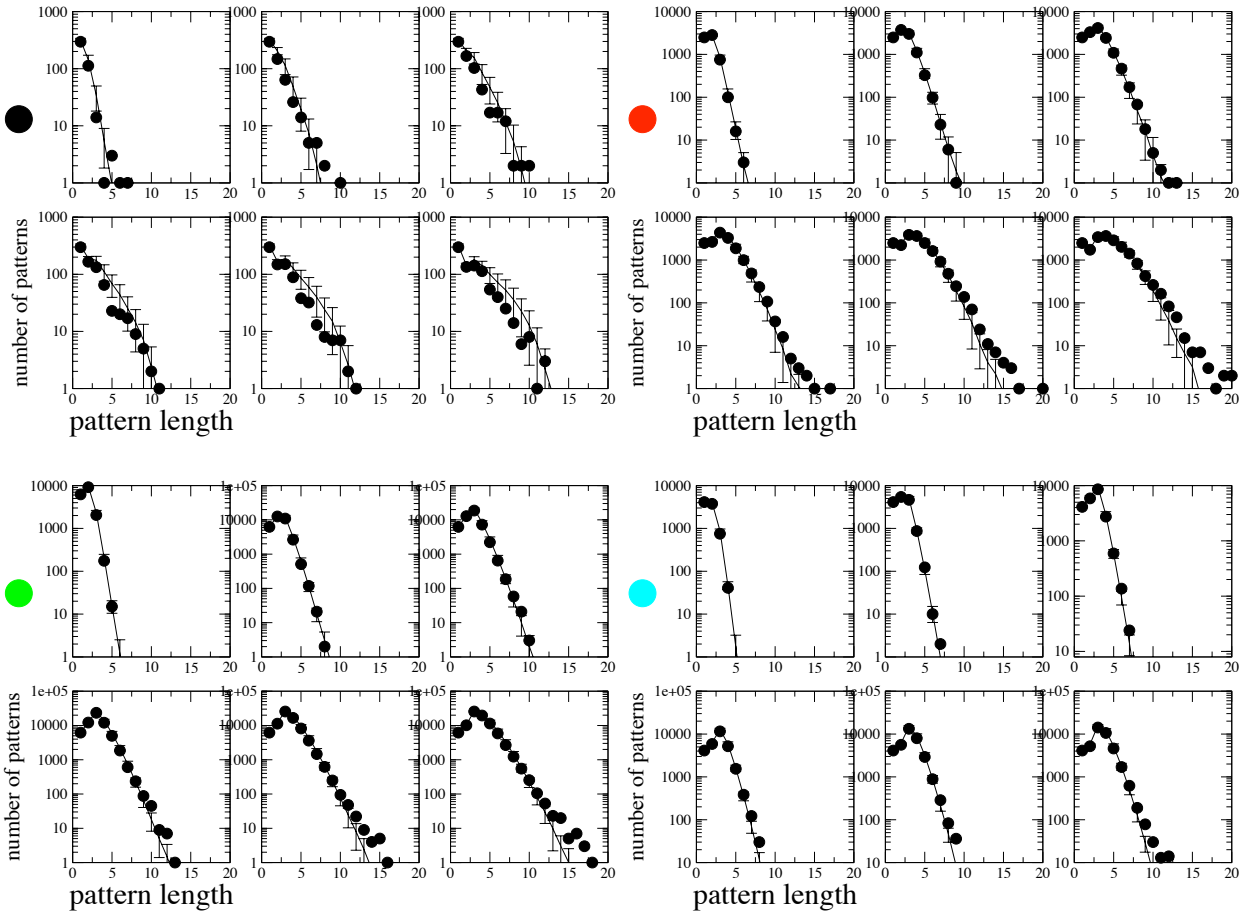

Fig. S.30: Pattern distributions. Circles: from experimental data. The corresponding data set is indicated by the symbol to the left of the figure. Lines: Results from 100 simulations of model 3. Error bars indicate one standard deviation. Shown are distributions for 6 values of the jitter, 0 to 5.

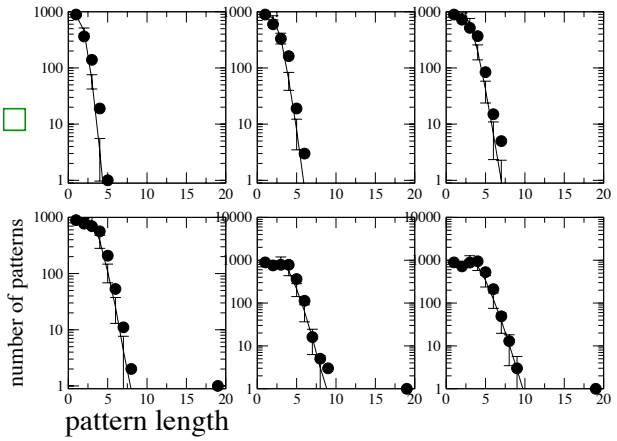

Fig. S.31: Pattern distributions. Circles: from experimental data. The corresponding data set is indicated by the symbol to the left of the figure. Lines: Results from 100 simulations of model 3. Error bars indicate one standard deviation. Shown are distributions for 6 values of the jitter, 0 to 5.

6.4 Model 4: Non-stationary stochastic model with interactions.

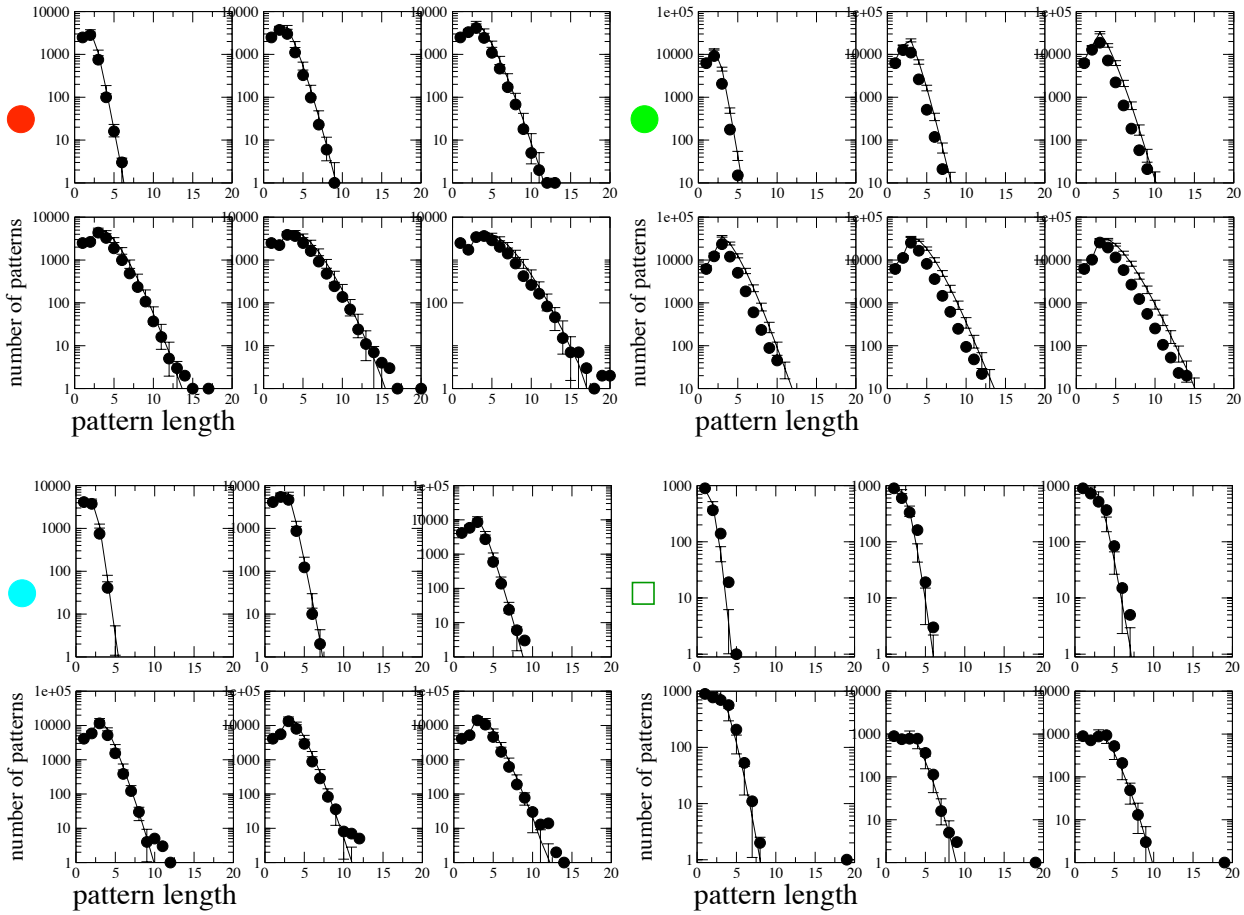

Fig. S.32: Pattern distributions. Circles: from experimental data. The corresponding data set is indicated by the symbol to the left of the figure. Lines: Results from 100 simulations of model 4. Error bars indicate one standard deviation. Shown are distributions for 6 values of the jitter, 0 to 5.

6.5 Randomized network 1: Randomization within full matrix.

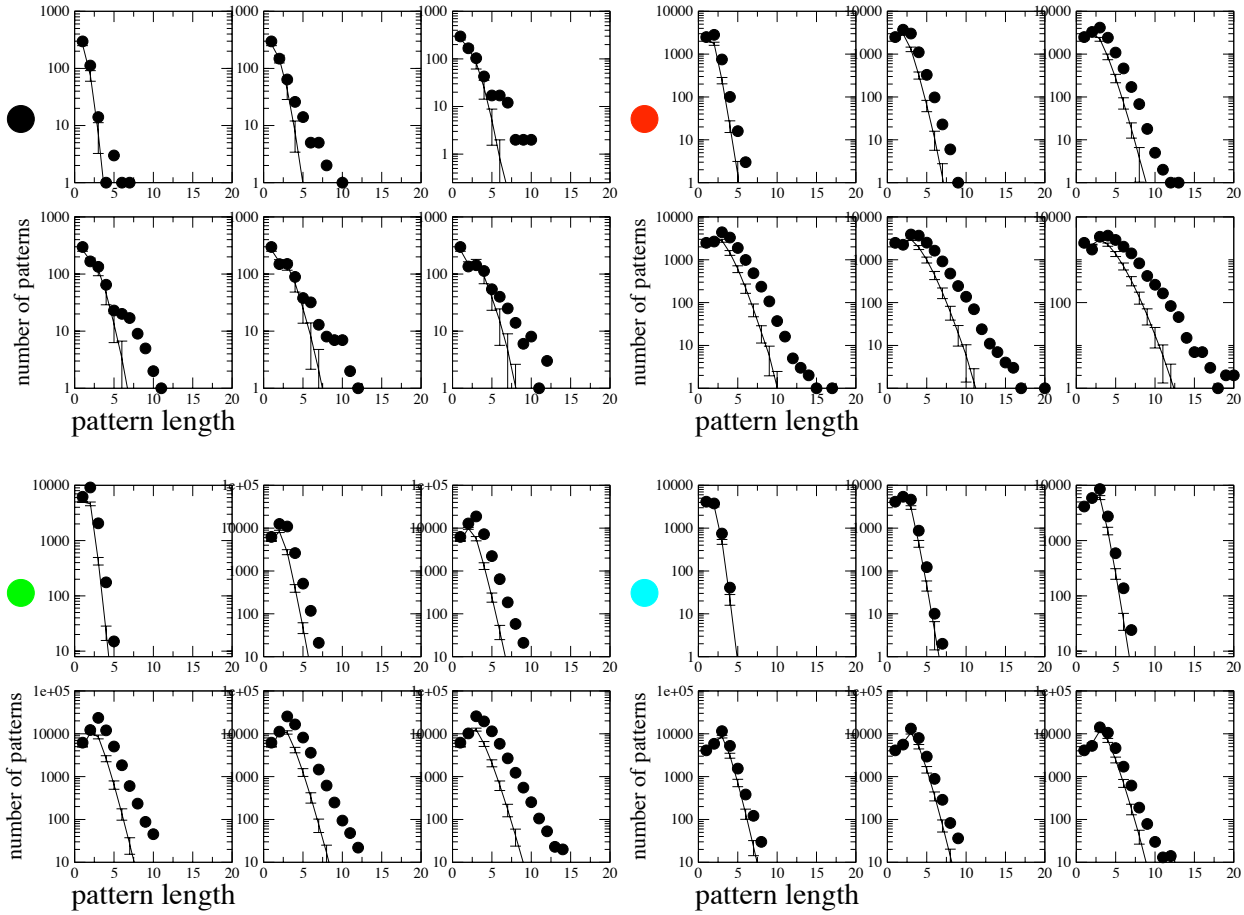

Fig. S.33: Pattern distributions. Circles: from experimental data. The corresponding data set is indicated by the symbol to the left of the figure. Lines: Results from 100 simulations of the best fit model with randomized connections. Error bars indicate one standard deviation. Shown are distributions for 6 values of the jitter, 0 to 5.

6.6 Randomized network 2: Randomization within connected sub-graph.

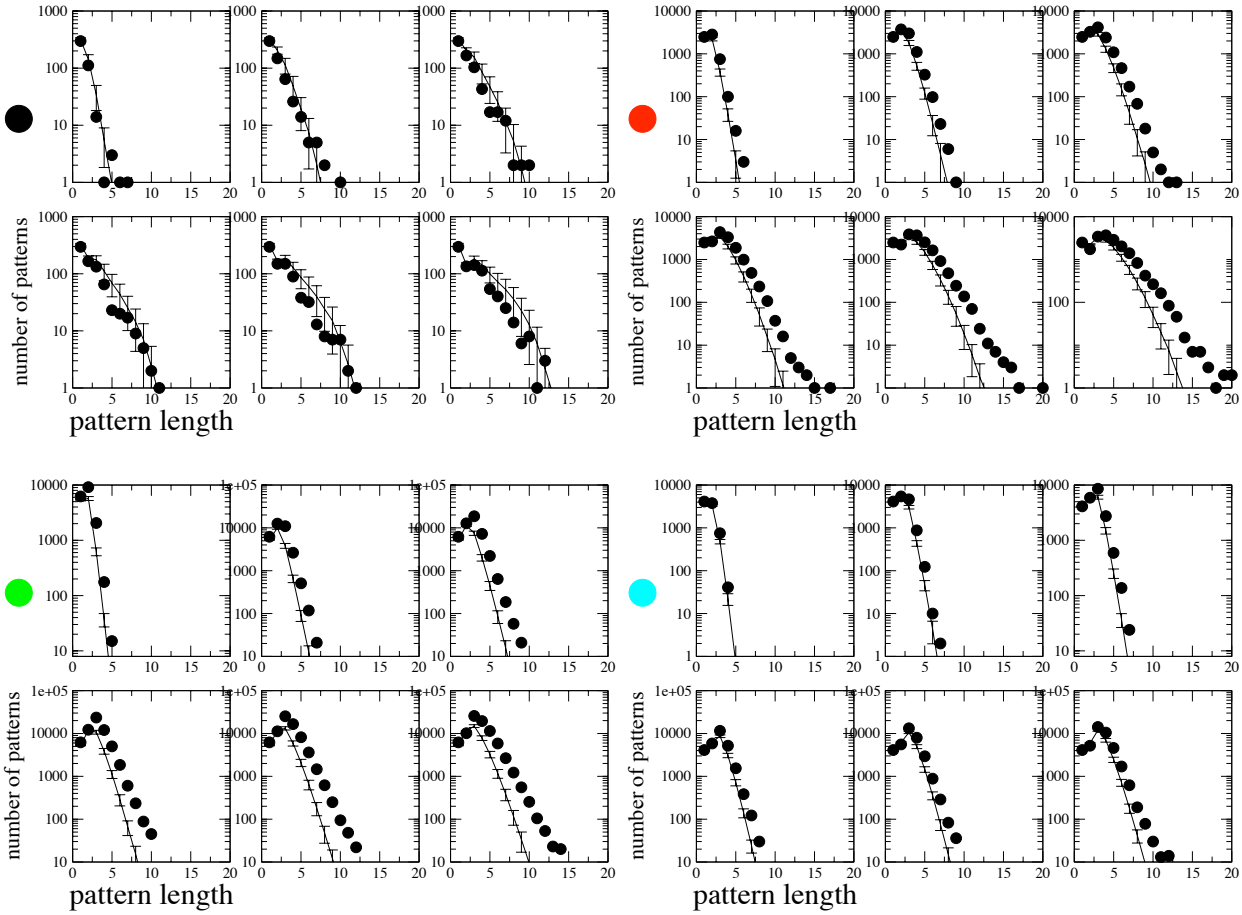

Fig. S.34: Pattern distributions. Circles: from experimental data. The corresponding data set is indicated by the symbol to the left of the figure. Lines: Results from 100 simulations of the best fit model with connections randomized within the connected sub-graph. Error bars indicate one standard deviation. Shown are distributions for 6 values of the jitter, 0 to 5.

6.7 Randomized network 3: Randomization keeping degree distribution.

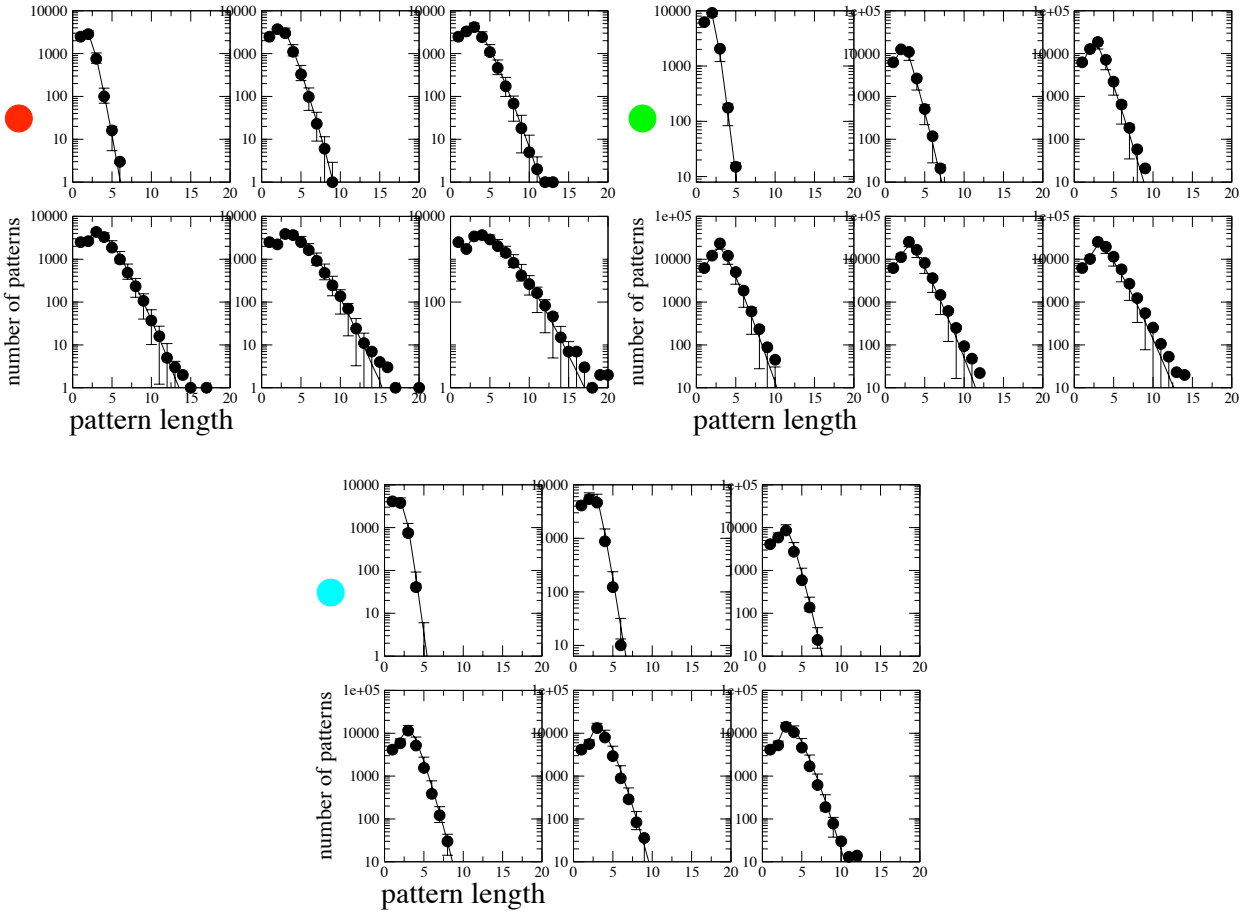

Fig. S.35: Pattern distributions. Circles: from experimental data. The corresponding data set is indicated by the symbol to the left of the figure. Lines: Results from 100 simulations of the best fit model with connections randomized within the connected sub-graph and in- and out- degree distributions kept intact. Error bars indicate one standard deviation. Shown are distributions for 6 values of the jitter, 0 to 5.